Hindawi
Adsorption Science & Technology
Volume 2022, Article ID 8625489, 22 pages
https://doi.org/10.1155/2022/8625489

Research Article

Removal of Hexavalent Chromium from Aqueous Solutions Using Natural Zeolite Coated with Magnetic Nanoparticles: Optimization, Kinetics, and Equilibrium Studies

Mohammed Asanu,[1] Dejene Beyene ,[2] and Adisu Befekadu[2]

[1]*College of Engineering and Technology, Bule Hora University, Department of Chemical Engineering, P.O. Box: 144, Ethiopia*
[2]*Faculty of Civil and Environmental Engineering, Jimma University, Jimma Institute of Technology, P.O. Box: 378, Ethiopia*

Correspondence should be addressed to Dejene Beyene; dejene.beyene@ju.edu.et

Received 23 March 2022; Revised 15 June 2022; Accepted 20 June 2022; Published 5 July 2022

Academic Editor: Walid Oueslati

Stringent discharge limits, high costs, and low removal efficiency of the conventional treatment methods are facing challenges to handle industrial effluents containing heavy metals. The objective of this study was to use a recoverable magnetic zeolite to remove Cr(VI) from aqueous solution. The study investigated the application of nanotechnology to improve surface properties, recoverability, and adsorptive capacity of natural zeolite and the CCD-RSM-based optimization of adsorption process variables. Natural zeolites coated with various fractions of magnetic nanoparticles (25%, 33.33%, 50%, and 75%) were investigated for surface characters, adsorption capacity, removal efficiency, and recoverability. Natural zeolite coated with 33.33% (MZ33) was found a better adsorbent in terms of surface characters, adsorption capacity, and removal efficiency. Thirty batch adsorption experiments designed with CCD were carried out in order to optimize adsorption process variables using response surface methodology (RSM). It was found that adsorbent dose = 2 g/L, contact time = 75 min, initial Cr(VI) concentration = 10 mg/L, and solution pH = 1.5 were the optimum conditions to achieve 93.57% Cr(VI) removal, which is very close to the experimental result of 94.88%. The adsorption isotherm determined from the operating parameters revealed that experimental data fit to the Langmuir isotherm model with $R^2 = 0.9966$ and maximum adsorption capacity = 43.933 mg/g. This proved that the adsorption of Cr(VI) on magnetic zeolite involved monolayer adsorption on the active sites. The separation factor, R_L, value lies between 0 and 1 indicating that adsorption of Cr(VI) on the magnetic zeolite is favorable. The adsorption kinetics study follows pseudo-first order in the removal of Cr(VI). FTIR analysis of magnetic zeolite revealed the presence of numerous functional groups participating in Cr(VI) adsorption. The current study confirmed that magnetic zeolite is a cost-effective and favorable material for the removal of Cr(VI) from aqueous solution.

1. Introduction

The incredible increase in the use of heavy metals in many industrial applications over the past decades has resulted in the flux of these metals in the environment [1]. Water polluted with heavy metals is a serious problem as these metals tend to persist and accumulate in the environment [2–4]. Municipal wastes, metal plating facilities, mining operations, effluents from fertilizer, tannery, and battery and paper industries are the major sources of heavy metals pollution [5]. Heavy metals are the most harmful to human health due to their physiological and neurological effects [6]. The toxic effects of heavy metal on human health come as the results of exposure through food, medications, environment, and occupation [4, 7]. Discharging heavy metals to water bodies beyond permissible limit is hazardous due to their toxicity, accumulation in the food chain, and persistence in the environment [5].

Chromium is a heavy metal that occurs naturally in water, sediments, rocks, soils, plants, animals, and volcanic emissions [8]. It exists in a number of oxidation states though only Cr(III) and Cr(VI) are stable in aqueous solution [9]. At trace level, Cr(III) is considered an essential nutrient for organisms,

whereas Cr(VI) is poisonous, carcinogenic, teratogenic, and mutagenic to biological systems [10, 11]. As the result of intensive use of chromium salts in many industrial applications, Cr(VI) is a common pollutant in many industrial effluents [1, 12]. Cr(VI) discharged with industrial effluents cause a serious pollution problems [13]. The necessity of treating wastewater containing Cr(VI) before discharged into the environment is due to the fact that it is highly soluble and mobile with deleterious health and environmental impacts [4]. The chronic effects of Cr(VI) include nerve paralysis, kidney and liver damage, dermatitis and respiratory impairments [7], genetic mutation, anemia, weakened immune system, and change of blood chemistry [1, 14]. The major sources of Cr(VI) in the aquatic environment are effluents discharged from electroplating, tanning, mining, fertilizer, and paint production industries [1]. In order to prevent pollution of water bodies with Cr(VI), its removal to a permissible level must be a top priority [4]. The World Health Organization (WHO) and Environmental Protection Agency (EPA) have set permissible limits for the discharge of heavy metals to reduce pollution of water bodies (Table 1). Accordingly, the permissible limit of Cr(VI) discharged to surface water is 0.10 mg/L, while it is 0.05 mg/L for drinking water which can be achieved through the proper treatment of the wastewater containing Cr(VI) before discharged to the environment [15].

Different treatment techniques such as chemical precipitation, electrodialysis, solvent extraction, reduction, coagulation-flocculation, ion exchange, adsorption, oxidation, membrane filtration, constructed wetland, biological treatment, electrochemical deposition, and chemical immobilization have been used to remove heavy metals from industrial effluents [16, 17]. However, most of these techniques have been found to be inefficient and not cost-effective, energy intensive, generate highly toxic sludge, and require expensive equipment [4, 9]. Among these techniques, adsorption is considered the best alternative treatment process owning to flexibility and simplicity of design, high removal efficiency, availability of different low-cost adsorbents, and ease of operation [18]. Adsorption processes with different types of natural and synthetic adsorbents such as low-cost activated carbon, industrial wastes, and activated carbon from low-cost agricultural and biowastes [19] have been found promising option for the removal of heavy metals from industrial effluents [3, 9]. However, the adsorbent materials need to be environmentally friendly, used at large scale, and cheap to treat industrial effluent containing heavy metal ions [1].

Since recent times, natural zeolites have gained considerable attention for the adsorptive removal of various pollutants from industrial effluents owing to high adsorption capacity and efficiency, highly specific surface area, ion exchange capacity, low cost, high chemical stability, and abundance [6]. Due to their superior properties, zeolites have been used for the removal of various contaminants such as phenol [20], dyes [21–23], and heavy metals [18] from various industrial effluents. Filtration and centrifugation techniques have been used to recover the natural zeolite after the adsorption process. However, such techniques have been found impractical, time-consuming, and costly to be used on large-scale industrial applications [24]. Separations of adsorbents from the solutions after the adsorption process and formation of secondary pollutant remain the major problems to be resolved.

Table 1: Maximum discharge limits of some heavy metals in water and wastewater (mg/L).

Heavy metal	Maximum contaminant limit (mg/L)	
	Water	Wastewater
Chromium	0.05	0.10
Mercury	0.001	0.00003
Arsenic	0.02	0.05
Cadmium	0.005	0.01
Lead	0.01	0.006
Nickel	0.02	0.20
Zinc	5.0	0.80
Copper	1.0	0.025

Various efforts have been made to improve the adsorption capacity and properties of adsorbent materials [25]. The use of adsorbents coated with magnetic nanoparticles for the treatment of wastewater contaminated with heavy metals has been considered an option to increase adsorption capacity and reuse of the adsorbents [1]. The development and use of a highly efficient, novel, robust, and cost-effective adsorbent for the removal of heavy metals from industrial effluents must be a prime issue to control pollutions. The adsorbents must possess high internal volume accessible to the adsorbates and good mechanical properties such as strength and resistance to destruction and appropriate particle size. The surface area, pore size distribution, and nature of pores of adsorbents determine the type of adsorption process. There is a need to improve the adsorption capacity, recoverability, and adsorption efficiency of natural zeolites to use them as an adsorbent for the removal of Cr(VI) from aqueous solution. One method to improve the economic, recoverability, and surface properties of natural zeolite is through transforming it to magnetic nanomaterial [10, 26, 27]. The magnetic nanomaterial need to possess easy recover, unique large surface areas, well-defined pore sizes, high pore volume, and great diversity in surface functionalization in order to alleviate problems associated with the use of natural zeolite [27–29]. Natural zeolites can be magnetized via co-precipitation [30, 31] and impregnation [32] techniques. Co-precipitation is the process of precipitating magnetic nanoparticles (Fe_3O_4) on natural zeolite surfaces using a mixture of Fe(II) and Fe(III) ions under alkaline condition [6, 28], while impregnation involves physical interaction between powdered natural zeolite suspended in water and magnetic nanoparticles (Fe_3O_4) under constant stirring [6, 26]. Literature survey reveals that co-precipitation results in magnetic zeolite with better surface and pore characters might be due to the fact that interaction between the natural zeolite powder and Fe_3O_4 results in a better dispersion on the zeolite surface. Meanwhile, the least dispersion of Fe_3O_4 particles on the zeolite surface during the impregnation process might be due to the fact that interaction between Fe_3O_4 and natural zeolite powder involves only physical interaction [33].

Adsorption is a mass transfer process in which an adsorbate moves from solution onto the surface of the adsorbent and interact with it via physical or chemical forces. Weak and nonspecific physical forces bind adsorbate molecules to the adsorbent surface using Van der Waals, dispersion interactions, and hydrogen bonds, while the specific chemical forces bind the adsorbate to adsorbent surface through the covalent or electrostatic interactions. The adsorption capacity of the adsorbent depends on its chemical properties such as degree of surface ionization, functional groups, and change upon contact with the solution. The presence of active functional groups on the surface of the adsorbent allows less reversible chemical interactions than physical interactions. The requirement of an efficient adsorbent for the removal of heavy metals from aqueous media includes cost-effectiveness, large surface area, pore size distribution, presence of functional group, and polarity [34].

A design of an efficient and a reliable adsorption process for the removal of heavy metals from aqueous media depends on adsorption kinetics data which explain the adsorption process and method as well as the speed at which adsorption sites are occupied and the number of vacant sites. The ability of various adsorbents is usually derived from adsorption kinetics. Adsorption kinetic models give adsorption mechanisms and rate controlling steps of adsorption process [34]. The rate of removal of a heavy metal depends on the physical or chemical properties of the adsorbent and the various variables affecting the adsorption process such as contact time, solution pH, initial metal concentration, and adsorbent dosage. The rate of adsorption process is usually studied using pseudo-first-order (PFO) and pseudo-second-order (PSO) kinetic models. The PSO model assumes that the rate of adsorption of an adsorbate is proportional to the available vacant sites on the adsorbent surface.

Intraparticle diffusion tries to identify the possible rate controlling step. The adsorbate transport from the bulk solution to the internal active sites of any porous adsorbent is often controlled by three-step process in which the slow process is the rate-limiting step [29]. If the linear plot of the amounts of adsorbate adsorbed at any instant of time (q_t) against square root of the time $(t^{0.5})$ does not pass through the origin, the intraparticle diffusion is not the only rate limiting step, and adsorption may be controlled by more than one process. These linear plots may be divided into multilinearity correlations, revealing that three steps occurred throughout the entire adsorption process [29]. The first linear part can be attributed to the transfer of adsorbate molecules from the solution to the external surface of the adsorbent via film diffusion. The second linear part indicates progressive adsorption where the intraparticle diffusion is the rate limiting step. The third part is attributed to the final equilibrium in which the process of intraparticle diffusion begins to slow down owing to the very low adsorbate concentrations remaining in solution [35].

The optimal adsorption capacity and interactions between adsorbents and adsorbate are commonly determined from adsorption isotherm models. Adsorption isotherms are mathematical models that relate the distribution of heavy metal ions between solution and adsorbent at equilibrium. The distribution of adsorbate between solution and adsorbent depends upon the nature of the adsorbent (i.e., whether it is homogeneous or heterogeneous) and the bond between the adsorbent and adsorbate. Langmuir and Freundlich adsorption isotherms are the most commonly used isotherm models. The Langmuir isotherm assumes that all binding sites of the adsorbent have an equal affinity which creates monolayer adsorbate molecules on the adsorbent surface, while the Freundlich isotherm involves heterogeneous surfaces having different affinities for the adsorbate molecules [34].

Optimization of adsorption process variables through the traditional approach is costly, time-consuming, and laborious and requires a large number of experiments. The limitations of the traditional approach can be solved using the central composite design (CCD) method of response surface methodology (RSM) which lowers the number of experiments and examine the effect of individual variables and their interactions on the response (removal efficiency). The RSM is a simple, effective, and low-cost statistical and mathematical model to analyze data, build a model, and evaluate the effects of independent variables on dependent variable to draw a reliable conclusions [36]. There are two main types of response surface designs: CCD and Box-Behnken designs (BBDs). The CCD is the most widely used statistical tools to design the effects of independent variables on the response [37]. It is often used when the design calls for sequential experimentation and needs to include information from factorial experiments, and the experimental runs embrace the extreme settings. On the other hand, BBDs have fewer design points than CCD and can estimate the first and second order coefficients but cannot embrace the factorial experimental runs. BBDs always have 3 levels per factor [38]. The CCD is used for the current study to design adsorption experiments, and model the linear, interactive, and quadratic effects of the four independent variables at five levels (- α, -1, 0, +1, and +α) on the dependent variable (Cr(VI) removal) as BBD cannot entertain factorial experimental runs, estimate five levels per factor, and cannot include extreme experimental points. The experimental results were analyzed by response surface regression [39], and the optimal condition for Cr(VI) adsorption was estimated using a second order model equation [40].

Hexavalent chromium was chosen to study adsorption capacity of magnetic zeolite since Cr(VI) is a hazardous pollutant owing to its high water solubility and toxicity. As far as the best knowledge of the authors is concerned, studies dealing with the use of magnetized zeolite for the removal of hexavalent chromium from aqueous solution have not been studied. In this study, the adsorptive capacity and recoverability of the magnetic zeolites were investigated. Studying surface characters of zeolite coated with various fractions of magnetic nanoparticles (Fe_3O_4) could improve its adsorption capacity and removal efficiency. Also, surface characters, removal efficiency and optimization of adsorption variables, adsorption isotherm, and kinetics studies were conducted.

2. Material and Methods

2.1. Chemicals and Equipment. A powdered natural zeolite purchased from Neway Private Limited Company was magnetized and used as adsorbent to study the adsorptive removal of hexavalent chromium from aqueous solution. $FeCl_3.6H_2O$, $FeCl_2.4H_2O$, NH_3, and Na_2SO_3 were purchased from the same supplier and used to prepare magnetic zeolite-Fe_3O_4 adsorbent. A stock solution of Cr(VI) was prepared by dissolving potassium dichromate ($K_2Cr_2O_7$) in deionized water. Hydrochloric acid, NaOH, acetone, and ethanol were used to adjust solution pH and analysis Cr(VI). Shimadzu Fourier transform infrared (FTIR), BELSORP-mini device surface area analyzer, Turbid meter, and atomic absorption spectroscopy (AAS) were used to characterize and analysis the magnetic zeolite. The central composite design (CCD) of design expert® version 13 software was used to design adsorption experiments and analyze process parameters affecting the adsorptive removal of Cr(VI) from aqueous solution. The response surface methodology (RSM) software was used to optimize the various adsorption process variables.

2.2. Preparation of Magnetic Zeolite. The powdered natural zeolite was washed with deionized water and dried in the oven at 100 °C for 24 h and then packed in a plastic bag and labeled as natural zeolite (NZ). A recoverable adsorbent of magnetic zeolite (zeolite-Fe_3O_4) was prepared by co-precipitation of Fe III) and Fe(II) ions under alkaline condition (Figure 1). A 1.50 g of magnetic zeolite powder was added to 1.50 g of magnetic nanoparticles, and the mixture was stirred at the constant rate and heated to 80 °C for 3 h to obtain a well-homogenized mixture. The solution was continuously stirred before cooled to room temperature (25 °C). The resulting magnetic zeolite was repeatedly washed with deionized water until it achieves neutral pH. The magnetic zeolite was dried in an oven under vacuum for 12 h. This solid zeolite-Fe_3O_4 containing 50 w/w% of Fe_3O_4 fraction was designated as MZ50. The same procedure was used to prepare magnetic zeolite containing 25 w/w%, 33.33 w/w%, and 75 w/w% Fe_3O_4 fractions by changing the mass of natural zeolite to 4.50 g, 3.0 g, and 0.50 g, respectively. The resulting magnetic zeolites were, respectively, labeled as MZ25, MZ33.33, and MZ75 (the numbers indicate Fe_3O_4 fractions contained in the magnetic zeolite). The magnetic zeolite-Fe_3O_4 was ground and sieved through a 250 mesh, characterized, and used for absorptive removal of Cr(VI) from aqueous solution.

2.3. Effects of Fe_3O_4 Fractions on the Surface Characters and Recoverability of Magnetic Zeolites. The effects of various Fe_3O_4 fractions on surface characters such as pore diameters, surface area, and pore volume and recoverability after adsorption process of the magnetic zeolite were studied. The magnetic zeolites with various Fe_3O_4 fractions were tested for their Cr(VI) adsorption capacity and recoverability to select the best magnetic zeolite. The degree of dispersion of magnetic nanoparticles on the surface of zeolite was studied by FTIR spectroscopy. Fourier transform infrared (FTIR) spectra were used to detect the interaction between Fe_3O_4 and zeolite surface structure. The initial and final concentrations of Cr(VI) ions in solution were measured using AAS. The turbidity of the filtrates from which MZ25, MZ33, MZ50, and MZ75 have been separated magnetically was quantitatively measured to correlate with the improvement in the recoverability of magnetic zeolite-Fe_3O_4. Higher turbidity indicates lower clarity of the filtrate, which in turn indicates the lower recoverability of the magnetic zeolite [33].

2.4. Adsorption Experiments and Experimental Design Using RSM-CCD. Adsorption process can be influenced by factors such as solution pH, contact time, adsorbent dosage, adsorbate initial concentration, co-existing ions, temperature, and agitation speed. The conventional method of process optimization is not only time-consuming and costly but also requires a large number of experiments. Experimental design allows maximum adsorption efficiency and optimization of independent variables with minimum errors and costs using the least number of experimental runs. Response surface methodology (RSM) is an effective tool to study the effects of variables and their interactions and optimize process variables. In this study, the RSM was used to optimize adsorption process variables and effects of variables interactions on the removal of Cr(VI) from aqueous solution using the recoverable magnetic zeolite. Adsorption experiments were conducted according to 2^n complete factorial for the four variables with a total of 30 experimental runs ($2^n + 2n + CP$), where n is number of variables, four in this case, and CP is the number of experiments at center point. Each variable was allowed to vary over five levels ($-\alpha$, -1, 0, +1, and $+\alpha$). Sixteen factorial (2^n) and 8 axial (2n) and 6 center point experimental runs were conducted (Table 2). The distance of axial points ($\pm\alpha$) to center point (CP) is calculated as follows [41, 42]:

$$\pm\alpha = \sqrt[4]{2^n}. \quad (1)$$

In order to estimate and evaluate test error and measure a lack of fit, central points were selected as a means [38]. Process variables and their ranges were determined based on the single factor experimental analysis and previous studies. Accordingly, the lowest and highest levels for coded levels of factors were −2 and +2, respectively. The axial points were fixed at ($\pm\alpha$, 0, 0, 0), (0, $\pm\alpha$, 0, 0), (0, 0, $\pm\alpha$, 0), and (0, 0, 0, $\pm\alpha$) for the four process variables.

2.5. Adsorption of Cr(VI) from Aqueous Solution Using the Magnetic Zeolite. CCD is widely used to approximate coefficients in a mathematical form and predicts reaction and validation of method. In this study, batch adsorption experiments designed by CCD were conducted at 150 revolution per minute (rpm) and temperature of 25 °C in order to investigate factors affecting the adsorption of Cr(VI) on magnetic zeolite from aqueous solution. A stock solution of Cr(VI) was prepared by dissolving exact quantities of potassium dichromate ($K_2Cr_2O_7$) in deionized water. Solutions of different Cr(VI) concentrations were prepared by

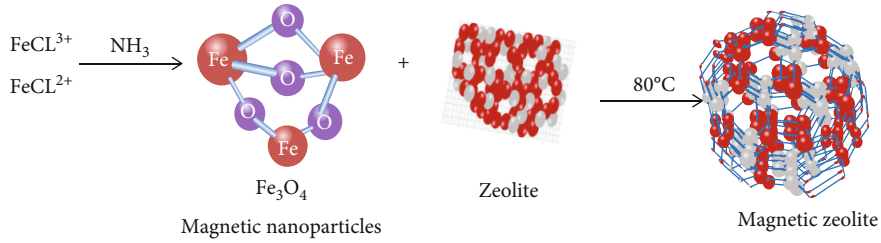

Figure 1: The schematics of magnetic zeolite-Fe_3O_4 preparation by co-precipitation technique.

Table 2: The actual and coded levels of adsorption process variables.

Factor	Symbol	Unit	Coded level				
			$-\alpha$	-1	0	$+1$	$+\alpha$
			Actual level				
Adsorbent dose	A	g/L	0.4	0.8	1.2	1.6	2.0
Contact time	B	Min	15	30	45	60	75
Initial Cr(VI) concentration	C	mg/L	10	30	50	70	90
pH	D	—	1.5	3	4.5	6	7.5

diluting the stock solution with suitable volume of deionized water [4]. A desired quantity (150 g) of magnetic zeolite (MZ50) was added to a known concentration (150 mg/L) of Cr(VI) ions and pH into a flask and kept in a shaker at fixed agitation speed (150 rpm) for various time intervals. After the mixture was shaken for a predetermined time, the magnetic zeolite adsorbent was recovered using a bar magnet, and the filtrate was analyzed using AAS to determine Cr(VI) concentration left behind in the solution. The same procedure was used for investigating adsorptive removal of Cr(VI) using magnetic zeolites MZ25, MZ33, and MZ75. The experiment for each type of magnetic zeolites was conducted in triplicate, and magnetic zeolite that has shown better performance and properties was used for adsorption process at various adsorbent doses, solution pH, contact time, and adsorbate initial concentrations. The pH of the solution was adjusted using 0.10 N NaOH/0.10 N HCl as desired to maintain the buffer conditions. The differences in concentration of Cr(VI) before and after adsorption were calculated to find out the amount of Cr(VI) adsorbed by the magnetic zeolite. The adsorption efficiency (R%) and adsorption capacity q_e (mg/g) of the magnetic zeolite are determined [4]:

$$R(\%) = \frac{C_{0-C_e}}{C_e} x100,$$
$$q_e\left(\frac{mg}{g}\right) = \frac{C_{0-C_e}}{m} V, \quad (2)$$

where C_o and C_e are, respectively, the initial and equilibrium concentrations of Cr(VI) ions (mg/L), V is the solution volume (L), R is the adsorption efficiency (%), m is the adsorbent mass (g), and q_e is the adsorption capacity (mg/g).

2.6. Adsorption Isotherm and Kinetic Studies. The adsorption isotherm indicates how the adsorbate molecules distribute between the liquid and solid phases at equilibrium. In order to optimize the design of an adsorption system, it is important to establish the most appropriate correlation for the equilibrium concentrations [43]. In the current study, the equilibrium isotherm was analyzed using the Langmuir and Freundlich isotherm models. The linear form of Langmuir isotherm is given in Equation (3), while the linear Freundlich isotherm is shown in Equation (4). In the Langmuir isotherm model, C_e is the equilibrium concentration of adsorbate in solution after adsorption (mg/L), q_m (mg/g) is the maximum monolayer adsorption capacity, q_e is the amount adsorbate adsorbed per unit mass of adsorbent (mg/g) at equilibrium, and b (L/mg) is the adsorption equilibrium constant as the ratio of adsorption rate to desorption rate that indicates affinity and ability of adsorbent surface [9]. Meanwhile, in Freundlich isotherm model, K_F (mg/g) $(mg/L)^{1/nF}$ is the adsorption capacity constant, while n is the adsorption intensity which indicates the degree of difficulty for the adsorption process. If n exceeds 2 but <10, the adsorption process proceeds easily. On the other hand, the ability for adsorption process would be too weak if n <0.50 ([9];
[4]):

$$\frac{C_e}{q_e} = \frac{1}{q_m b} + \frac{C_e}{q_m}, \quad (3)$$

$$\log(q_e) = \frac{1}{n}\log(C_e) + \log(K_F). \quad (4)$$

The mass transfer from the solution to the adsorption sites within the adsorbent is constrained by mass transfer resistances that determine the time required to reach the equilibrium. Parameters for adsorption kinetics were determined

based on contact time variation data via pseudo-first-order and pseudo-second-order equations [44]. The kinetic parameters obtained were adsorption capacity at equilibrium (q_e) and adsorption rate constant (K_F). The adsorption kinetics for Cr(VI) ions that well fit were inferred from coefficient of determination (R^2). The adsorption capacity and adsorption rate constant show good ability of adsorbent and potential of the adsorbent.

2.7. Data Analysis. The data generated were analyzed using origin pro software to compute standard deviation and linear regression values. The E-draw max software was used to draw the co-precipitation technique of making magnetic zeolite, while RSM was used to optimize adsorption process variables. A quadratic model was used to estimate the interaction between the response and the four independent variables. The statistical significance of the quadratic model was determined based on the lack of fit (LOF) test, coefficient of determination (R^2), and adjusted coefficient of determination (R^2 adj) between experimental and predicted data. Pareto analysis was carried to calculate the percentage effect of each independent variable on the removal of Cr(VI) from aqueous solution. AAS, FTIR, BELSORP-mini device surface area analyzer, and pHzc were used to characterize the magnetic zeolites.

3. Results and Discussion

3.1. Characterization of Magnetic Zeolite. The properties of zeolite depend on its physical, chemical, and mineralogical characteristics which in turn influence the overall adsorption process [33]. Surface characters such as pore diameters, surface area, and pore volume of the magnetic zeolite containing various fractions of magnetic nanoparticles were studied (Table 3). Point of zero charge (Pzc) and FTIR were used to study the characteristics of raw (natural) and magnetic zeolite adsorbents. The pH value at which the net charge on the surface of a material becomes zero is known as the pHpzc of the material. The pH of zero charge (pHpzc) was determined by mixing magnetic zeolite with a solution of NaCl. The pH of each sample was adjusted to different values using HCl and NaOH solutions. After 24 h, the final pH of solutions was measured, and the point of intersection of final pH versus initial pH was recorded as pHpzc of the adsorbents. The result shows that magnetization decreases pore diameters but increases surface area and pore volumes. Reducing the pore diameter might be due to the filling of magnetic nanoparticles in the zeolite pores. This might be due to the fact that increasing Fe_3O_4 fraction gives smaller pore diameter by occupying the pores. The improvement in surface area indicates that magnetic particles also occupy active surface of the adsorbents. Although more magnetic particles loaded in the adsorbent contribute larger surface area, extra addition may form aggregate with larger size that reduces the surface area. The excess of magnetic nanoparticles increase pore volumes [33].

3.2. Determination of Point of Zero Charge (pHpzc). Solution pH plays a great role in adsorption of cations as it influences speciation and ionization of adsorbent active sites. The net charge of adsorbent surface may play a crucial role in adsorption processes, and characterization of protonation-deprotonation behavior of the adsorbent is very important in explaining the mechanism of adsorption [29]. The point of zero charge (pHpzc) determines the surface charge of the adsorbent at a given pH that suggests the possible electrostatic interactions between adsorbent and a species of heavy metal (adsorbate). The surface charge of the adsorbent is neutral at the solution pH equal to pHpzc. When the pH of the solution < pHpzc, the adsorbent reacts as a positively charged surface, and when it is > pHpzc, the adsorbent functions as a negatively charged surface [29, 45]. The intersection of the final pH curve is the function of initial pH curve with the bisector corresponds to the pH of adsorbent and is equal to point of zero charge (pHpzc) [19]. The adsorption of Cr(VI) ions by natural zeolite (NZ) and magnetic zeolite (MZ) increases with increase in pH. Each adsorbent can be explained by its pHpzc (Figure 2). If pH is higher than pHpzc, the net charge is negative, and adsorbent could interact with positive metal ions. It can be observe that the magnetic zeolite adsorbent can interact with metal positive ions such as Cr(VI). If the measured pH of the solution is lower than pHpzc, the net surface charge is positive, and positively charged surface (pH < pHpzc) tends to repulse cations in the solution and lower metal adsorption on adsorbent surface. Thus, at low pH, adsorptions of cations tend to be low. In the current study, the pHpzc values of natural zeolite (NZ), MZ25, MZ33.3, MZ50, and MZ75 were found to be 4.9, 3.47, 3.50, 3.64, and 3.76, respectively. The pHpzc of MZ is lower than that of NZ. At the same pH above their pHpzc, the positive charges on the surface of magnetic zeolite would be expected to be greater than NZ. Hence, cation adsorption onto MZ is expected to be higher than NZ at the same pH. The uptake of Cr(VI) by NZ, which is optimum at pH 4, was found to be 72.39% for NZ. The experiment conducted using magnetic zeolite prepared by co-precipitation for the adsorption of Cr(VI) gave the optimum condition at pH 3.5 with adsorptive removal of 90.2%. Experiments were performed at solution pH of 3.5 to avoid any possible hydroxide precipitation. The value of pHpzc on the surface of MZ75 was found to be 3.76 (Figure 3), indicating that Cr(VI) adsorption is favorable at pH value higher than pHpzc while adsorption of anion ($HCrO_4^-$) is favored at pH values lower than pHpzc. This suggests that adsorption of Cr(VI) is highly favorable at the pH value < 3.76 and this might be attributed to strong electrostatic attraction between

Table 3: Surface and pore characteristics of natural and magnetic zeolites.

Adsorbent type	Pore diameter (Å)	Surface area (m^2/g)	Pore volume (cm^3/g)
NZ (raw)	18.67	21.20	0.099
MZ (25%)	13.40	78.69	0.264
MZ (33.3%)	10.07	88.14	0.222
MZ (50%)	7.39	77.68	0.145
MZ (75%)	2.13	68.23	0.036

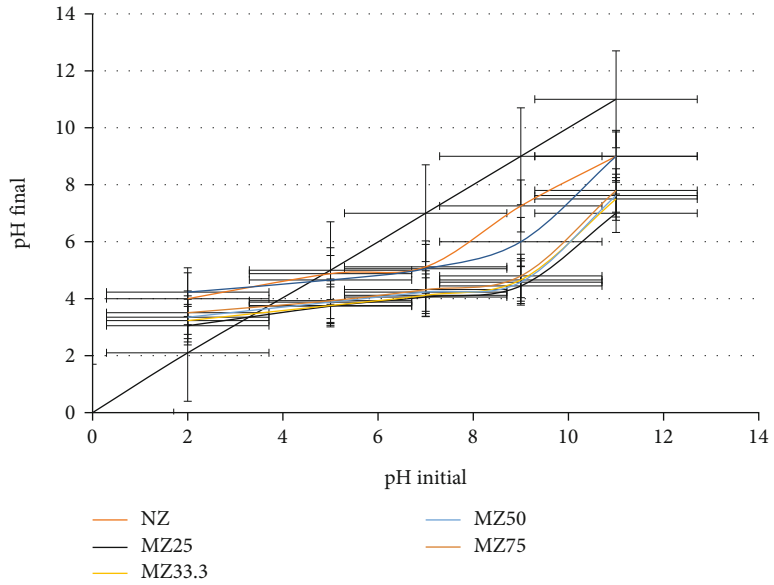

Figure 2: pH of zero charge of the natural and magnetic zeolites.

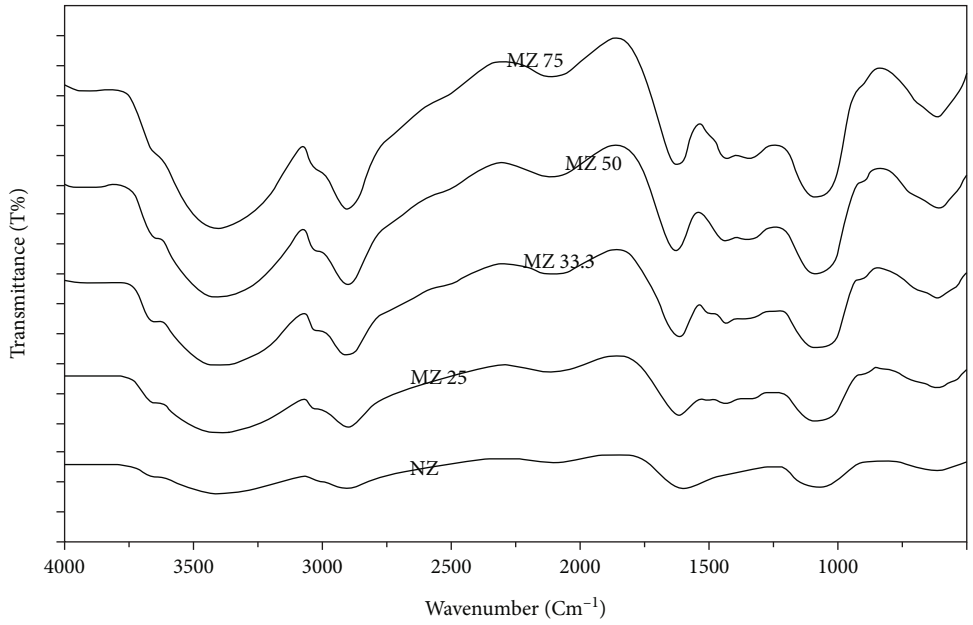

Figure 3: FTIR spectra of NZ, MZ25, MZ33, MZ50, and MZ75 adsorbents.

anion ($HCrO_4^-$) and protonated oxygen-containing functional groups (Si–O and Si-O-Al) present on the surface of the magnetic zeolite adsorbent. The finding of this study agrees with previous studies which found that higher adsorption of Cr(VI) is favorable at pH values 3–6 [33].

3.3. Fourier Transform Infrared Spectroscopy (FTIR) Analysis. FTIR spectra have been recorded to detect the interaction between Fe_3O_4 and natural zeolite structure (Figure 3). The spectra illustrate various peaks at which zeolite appear at different wavenumbers. Absorption band at 4000-3740 regions resent stretching bond of Si-OH.

Band region of 3740-3610 resent stretching bond of Si-OH-Al. Band region at 3425-3441 represents stretching vibration of O-H bonds of water molecules in zeolites. This band overlaps with the stretching vibration of the O-H bonds of hydroxyl terminal group in the zeolite. Absorption band at 3441-1635 regions indicates the bending vibration of the H–O–H bond from water (Table 4). The sharp and strong absorption band at 1635-1049 cm^{-1} corresponds to O-Si-O and O-Al-O asymmetry stretching, while the absorption band at 447-462 region might be due to the presence of the bending vibration of these bonds in the tetrahedral framework of zeolite. Furthermore, the absorption peaks of all magnetic zeolites

Table 4: Frequencies and functional groups on the surface of magnetic zeolite.

Frequencies (cm^{-1})	Bond	Functional group
4000-3740	Si-OH	Framework of zeolite
3740-3610	Si-OH-Al	Framework of zeolite
3425-3441	Stretching vibration of O-H	Water, hydroxyl zeolite
3441-1635	Bending vibration of the H–O–H	Water
1635-1049	O-Si-O/O-Al-O asymmetry stretching	Tetrahedral framework of zeolite
447-462	Bending vibration of O-Si-O/O-Al-O	Tetrahedral framework of zeolite
Magnetic nanoparticle (Fe_3O_4)		
1425	O-H vibrations	Fe_3O_4
570	Fe-O vibrations	Fe_3O_4

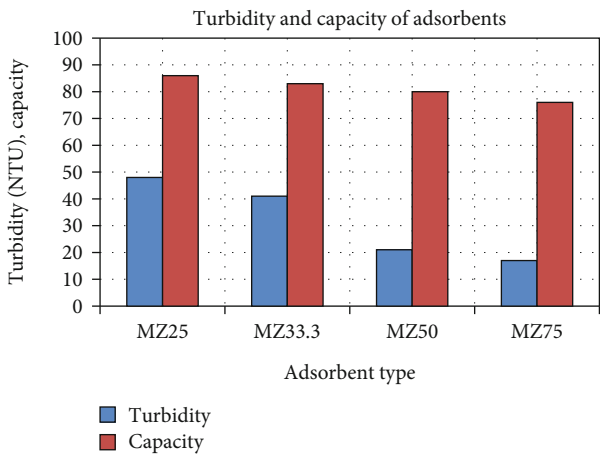

Figure 4: Turbidity of filtrate and adsorption capacity of magnetic zeolites.

reveal combination of peaks of zeolite and Fe_3O_4 nanoparticles. It suggests that Fe_3O_4 particles have covered the zeolite surface structure. In the spectra of magnetic zeolite, a new peak at around 1420 was observed which is believed to be due to Fe-O-Si bond. It indicates that in synthesizing magnetic zeolite, Fe atoms of Fe_3O_4 attach to Si-O of zeolite, indicating the successful coating of magnetic nanoparticles on the surface of zeolites.

3.4. Recoverability of the Magnetic Zeolite. The magnetic zeolite was separated magnetically from the magnetic zeolite and adsorbate solution mixture. Figure 4 shows the adsorption capacity of the adsorbents and turbidity of the filtrates that result from separation of each adsorbent after adsorption process. It is worthwhile to note that the higher turbidity, the lower clarity of the filtrate; hence, it demonstrates the reduced recoverability of the adsorbent. Increasing magnetic nanoparticles fraction on natural zeolite has improved the recoverability, but in divergence, it causes the adsorption capacity slightly reduced. The presence of Fe_3O_4 can contribute to the magnetic property of the adsorbents, allowing them easier to recover magnetically. At the same time, Fe_3O_4 particles cover some part of the zeolite surface that reduced the adsorbent active sites. Although more Fe_3O_4 fractions can extent the surface area of the adsorbents, it does not always enlarge the adsorption surface. The better recoverability has created by the better dispersion of Fe_3O_4 on the adsorbent. This data is in a good agreement with the turbidity of filtrate.

3.5. The Statistical Analysis and Model Fitting. The effects of adsorption process variables were studied in order to maximize the removal of Cr(VI) ions from aqueous solution using the magnetic zeolite. In order to obtain the maximum response (Cr(VI) removal) that satisfies all process variables, optimization was carried out using the Design Expert software version 13 State-Ease, Inc., USA (based on CCD). The CCD with five level-four factors of the software was used to design the 30 experimental runs, which cover the full ranges of the four independent process variables. The complete design matrix of the actual and coded levels and the experimental and predicted responses ((Cr(VI) removal) for the current study are shown in Table 5. The experimental results were optimized to enhance the removal of Cr(VI) ions by analyzing the influence of adsorbent dosage (0.40–2.0 g/L), contact time (15–75 min), initial Cr(VI) concentration (10–90 mg/L), and solution pH (1.5–7.5). The responses of the 30 experimental runs were fitted to a quadratic model equation which consists of an intercept, four linear terms (A, B, C, and D), four quadratic terms (A^2, B^2, C^2, and D^2), and six interaction terms (AB, AC, AD, BC, BD, and CD) to predict the response as function of coded variables:

$$Y = 56.87 + 1.22A + 9.16B - 5.59C - 5.86D + 2.35AB - 2.81AC - 1.69AD + 1.27BC - 0.72BD + 0.63CD - 0.36A^2 + 0.72B^2 + 2.48C^2 + 5.10D^2. \quad (5)$$

The analysis of variance (ANOVA) results for the quadratic regression model were used to determine the suitability and sufficiency of the model. The statistical significance of the quadratic model was determined using the lack of fit (LOF) of F test, coefficient of determination (R^2), and adjusted coefficient of determination (R^2 Adj) between experimental and predicted values [41]. The significance of each terms of the quadratic model equation was evaluated using p value. The p value signifies the probability of error and is used to confirm

Table 5: CCD based experimental design (actual and coded levels) and responses (removal efficiencies).

Run order	Design type	Actual levels			Coded levels					Removal efficiency (%)		
		Dose (g/L)	Time (min)	Cr(VI) conce (mg/L)	pH	A	B	C	D	Actual	Predicted	Residue
1	Center	1.2	45	50	4.5	0	0	0	0	55.74	56.28	-0.54
3		1.2	45	50	4.5	0	0	0	0	54.24	56.28	-2.04
7		1.2	45	50	4.5	0	0	0	0	57.65	56.28	1.37
10		1.2	45	50	4.5	0	0	0	0	57.27	56.28	0.99
11		1.2	45	50	4.5	0	0	0	0	55.36	56.28	-0.92
12		1.2	45	50	4.5	0	0	0	0	60.98	56.28	4.70
4	Factorial	0.8	60	70	3	-1	1	1	-1	73.25	73.15	0.10
5		0.8	60	30	3	-1	1	-1	-1	76.66	77.43	-0.77
8		1.6	30	30	3	1	-1	-1	-1	73.23	71.64	1.59
13		0.8	30	30	3	-1	-1	-1	-1	65.87	64.91	0.96
14		1.6	30	70	6	1	-1	1	1	39.81	38.64	1.17
15		1.6	30	30	6	1	-1	-1	1	57.92	56.72	1.20
16		0.8	60	70	6	-1	1	1	1	63.45	64.63	-1.18
17		0.8	30	70	6	-1	-1	1	1	49.91	49.91	0
18		0.8	30	70	3	-1	-1	1	-1	55.95	55.55	0.40
20		1.6	60	30	3	1	1	-1	-1	94.88	93.57	1.31
22		0.8	60	30	6	-1	1	-1	1	66.38	66.38	0
23		1.6	60	30	6	1	1	-1	1	75.76	75.76	0
24		1.6	60	70	3	1	1	1	-1	78.29	78.06	0.23
25		1.6	60	70	6	1	1	1	1	63.12	62.77	0.35
29		0.8	30	30	6	-1	-1	-1	1	56.92	56.75	0.17
30		1.6	30	70	3	1	-1	1	-1	52.35	51.04	1.31
2	Axial	0.4	45	50	4.5	-2	0	0	0	53.99	52.98	1.01
6		1.2	45	90	4.5	0	0	2	0	55.28	56.61	-1.33
9		2	45	50	4.5	2	0	0	0	55.13	57.85	-2.72
19		1.2	45	10	4.5	0	0	-2	0	76.59	77.97	-1.38
21		1.2	45	50	1.5	0	0	0	-2	87.28	88.99	-1.71
26		1.2	15	50	4.5	0	-2	0	0	38.88	41.43	-2.55
27		1.2	75	50	4.5	0	2	0	0	78.91	78.07	0.84
28		1.2	45	50	7.5	0	0	0	2	65.55	65.55	0

the significance of model terms. In this study, only model terms with p value < 0.05 were considered significant. Accordingly, all linear terms A (adsorbent dosage, p value = 0.0096), B (contact time, p value < 0.0001), C (initial Cr(VI) concentration, p value = 0.0003), D (solution pH, p value < 0.0001); the four interaction terms AB (interaction of adsorbent dosage and contact time, p value = 0.0003), AC (interaction of adsorbent dosage and initial Cr(VI) concentration, p value < 0.0001), AD (interaction of adsorbent dosage and solution pH), and BC (interaction of contact time and initial Cr(VI) concentration, p value = 0.0232); and two quadratic terms initial Cr(VI) concentration (C^2, p value < 0.0001) and solution pH (D^2, p value < 0.0001) were found statistically significant for the current study.

All terms containing contact time and pH interactions, initial Cr(VI) concentration and solution pH interaction, adsorbent dosage, and contact time quadratic terms were not significant ($p > 0.05$) (Table 6). The 3D response surface plots were drawn to depict the interaction effect of two variables, while the third variable kept at center point. The negative signs in the coefficients of model terms indicate an inverse relationship (no increase in efficiency as the factor level increases) between the response (Cr(VI) removal) and the independent variable, while positive signs indicate the synergistic effect (increasing factor level increases the removal efficiencies) between process variables and the response [39]. The magnitude of regression coefficients indicates the degree of significance of each independent variable for the removal of Cr(VI) from aqueous solution. Accordingly, B (contact time) is the most significant independent variable. The p value < 0.0001 of the model indicates that the model is suitable and statistically significant in predicting the removal of Cr(VI) at the 95% confidence level. Also, a p value < 0.0001 of the model indicates that the probability of obtaining a large F value due to noise is <0.01%. The lack of fit (LoF) of F test indicates that it describes sufficiently the

Table 6: ANOVA for quadratic model for removal of Cr(VI).

Source	Sum of square	DF	Mean squares	F value	p Value	Remark
Model	4773.64	14	340.97	84.21	**<0.0001**	Significant
A-adsorbent dosage	35.65	1	35.65	8.80	0.0096	
B-contact time	2014.65	1	2014.65	497.56	<0.0001	
C-initial concentration	749.40	1	749.40	185.08	<0.0001	
D-pH	824.50	1	824.50	203.63	<0.0001	
AB	88.60	1	88.60	21.88	0.0003	
AC	126.28	1	126.28	31.19	<0.0001	
AD	45.80	1	45.80	11.31	0.0043	
BC	25.88	1	25.88	6.39	0.0232	
BD	8.31	1	8.31	2.05	0.1725	
CD	6.39	1	6.39	1.58	0.2283	
A^2	3.64	1	3.64	0.90	0.3578	
B^2	14.19	1	14.19	3.50	0.0808	
C^2	168.60	1	168.60	41.64	<0.0001	
D^2	713.21	1	713.21	176.14	<0.0001	
Residual	60.74	15	4.05	—	—	
Lack of fit	32.60	10	3.26	0.5794	0.7837	Not significant
Pure error	28.13	5	5.63	—	—	
Total	4834.37	29	—	—	—	—

Table 7: Model summary statistics.

Source	SD	R^2	Adjusted R^2	Predicted R^2	Press	Remarks
Linear	6.96	0.7497	0.7096	0.6363	1758.06	
2FI	6.92	0.8120	0.7130	0.6729	1581.56	
Quadratic	2.01	0.9874	0.9757	0.9528	228.30	Suggested
Cubic	2.32	0.9922	0.9677	0.7058	1422.25	Aliased

Table 8: Model fit statistics for the removal of Cr(VI) ions.

Factor	Value
SD	2.01
Mean	63.22
CV (%)	3.18
R^2 (coefficient of determination)	0.9874
Adjusted R^2	0.9757
Predicted R^2	0.9528
Adequate precision	38.606

relationship between independent variables and dependent variable. LOF of F value for this study was found to be 0.5794, while the p value of the LOF was found to be 0.7837. The p value of the LOF > 0.05 indicates that there is a good fit between the model and experimental data. The F value of 84.21 along with the low p value (<0.0001) suggested that the established model was highly significant.

3.6. Model Selection and Fitting. In order to select model algorithm that fits well, the regression equation was solved using the Design Expert® 13 software to obtain optimal Cr(VI) removal for the four adsorption process variables. In order to predict results accurately and precisely, selection of an accurate model algorithm must be the first step [38]. Selection of model algorithm was based on fitness. The software suggested that model summary statistics (Table 7) revealed that the quadratic model can fit well in predicting the results accurately and precisely. This is because additional terms were significant and the model is not aliased (i.e., it could be used to describe the relationship between the response and interacting variables).

A high coefficient of determination value of $R^2 > 0.9$ for the model obtained via multiple regression analysis suggests that the independent variables were responsible for the majority of the variability. The quadratic model had a small standard deviation (SD = 2.01) and coefficient of determination ($R^2 = 0.9874$) with predicted coefficient of determination (pred $R^2 = 0.9528$) that is in a good agreement with adjusted coefficient of determination (adj $R^2 = 0.9677$).

The closeness of R^2 value to unity with smaller standard deviation indicates the suitability of the model in predicting the response (removal of Cr(VI)) precisely. However, a large value of R^2 does not always mean that the model is a good one, and such inference can only be made based on a high

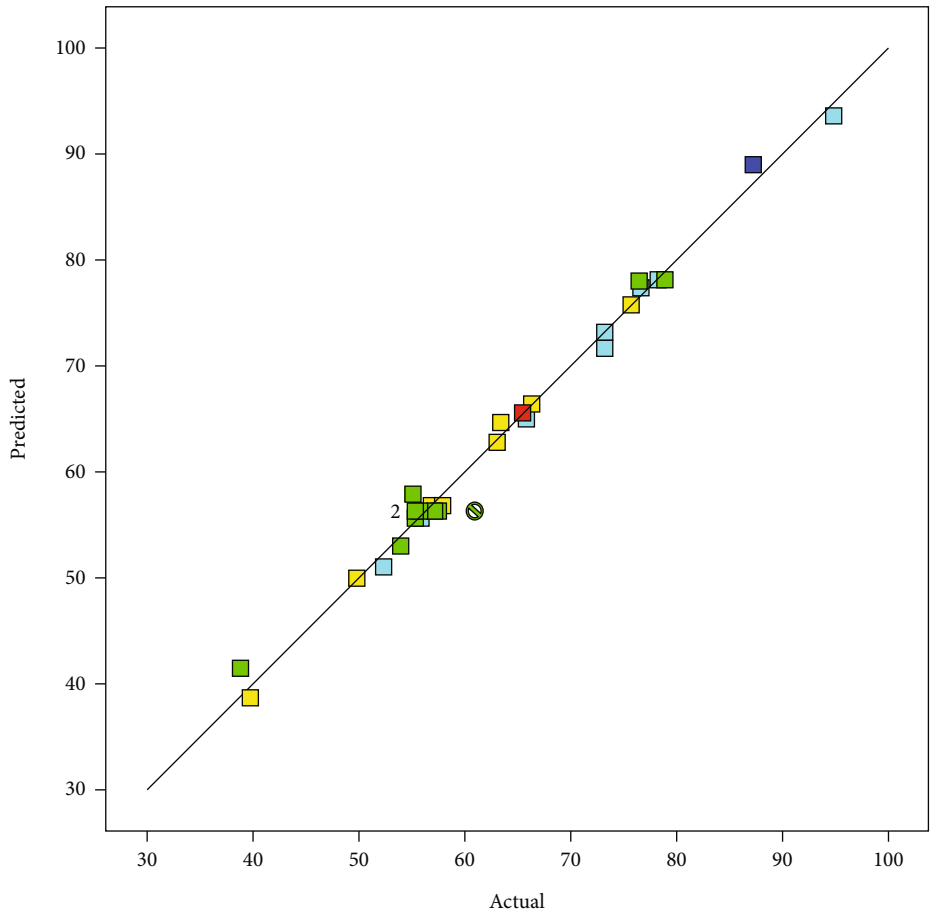

Figure 5: Predicted vs. actual values of response.

value of adjusted coefficient of determination (adj R^2). For the model to be in good agreement, the difference between adjusted R^2 and predicted R^2 should be within 20% [46, 47]. This requirement is satisfied in the current study because the difference between the values of adjusted R^2 and R^2 (equal to 0.0229 or 2.29%) is within 20%. This confirms that the model is highly significant and indicates a good agreement between the experimental and predicted data. The model adequate precision of response was >4.0, indicating a good agreement between the experimental and predicted values and high significance of the model [38, 41]. The predicted R^2 of 0.9528 shows that the model was adequate and offers 63.22% variability in predicting removal of Cr(VI) ions from aqueous solution. In addition, R^2, adjusted R^2 and predicted R^2 having values of 0.9874, 0.9757, and 0.9528, respectively, revealed that the predicted and experimental values are in good agreement (Table 8). The coefficient of variance (CV) is standard error ratio to mean value of experimental response. The higher the CV value, the lower the reliability of the experimental results. The CV value of 3.18% for the current study indicates a high precision and a good reliability of the experimental data. The insignificance of LOF of F test indicates that the model fits the data within the replicate variation. The model mean value for Cr(VI) removal using the magnetic zeolite adsorbent was 63.22.

The plot of predicted values vs. actual values shows that the predicted values closely fit the experimental results; hence, there is adequate correlation between the predicted and experimental data which indicate the adequacy of the model (Figure 5). A minimal divergence of points from the diagonal line indicates that the model equations can be used to show the interaction of the four independent variables. For high-quality agreement, the actual vs. predicted values should lie near Y = X line. The real Cr(VI) removal efficiency vs. predicted removal efficiency indicates the percentage. To test whether the data follows a normal distribution or not, a normal probability plot of the residue was employed. When the data points on the normal probability plot form a straight line, it indicates that the data are normally distributed, while departure from a straight line indicates departure from normal distribution of the residues. The data points forming approximately a straight line indicate that the data set is normally distributed and data are reliable (Figure 6). This indicated that Equation (4) is a suitable to describe the response (removal of Cr(VI from aqueous solution).

3.7. The Interactive Effect of Variables on the Cr(VI) Removal Efficiency. The magnetic zeolite with Fe_3O_4 fraction that has shown better recoverability, adsorption capacity, and removal efficiency was used to study the interactive effect of adsorption process variables on the removal of Cr(VI)

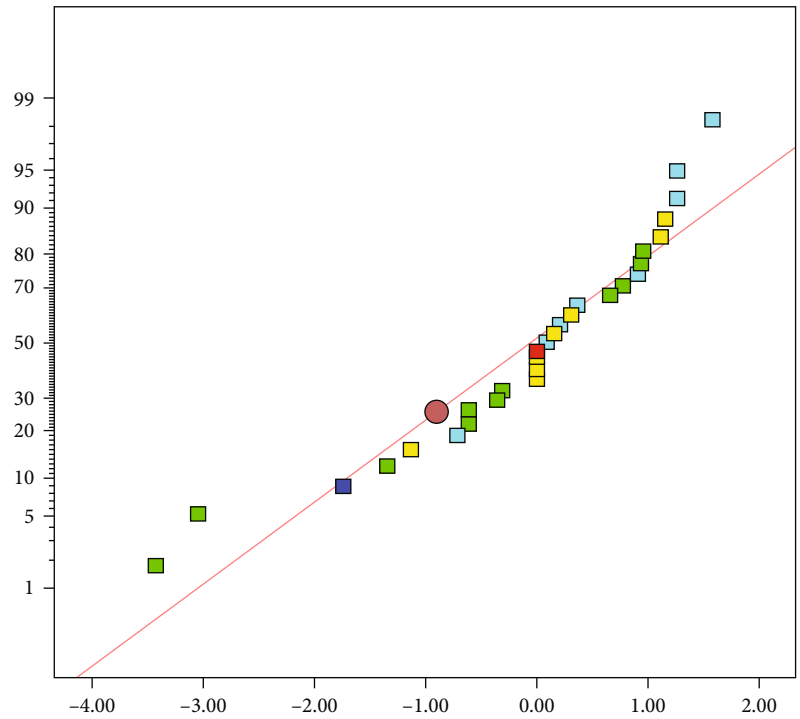

Figure 6: Normal probability plot.

from aqueous solution. Design Expert® 13 software was used to draw response surface plots using the regression model equation using the significant terms. As the individual plot does not show the interaction among process variables, three-dimensional (3D) response surface plots were drawn to show effect of variable interaction on the removal efficiency of Cr(VI). Three-dimensional response surface plots and ANOVA results were used to study interactive effect of studied variables on the removal efficiency of Cr(VI) and to determine the type of relationship between the variables. The three-dimensional response surface plots were drawn by combining two variables while keeping the third variable constant at the center point [35]. The interactive effects of independent variables (adsorbent dosage, contact time, initial Cr(VI) concentration, and solution pH) on the Cr(VI) removal using the magnetic zeolite are shown in Figures 7(a)–7(d). Based on the 95% confidence limit, only those variables with a p value < 0.05 were considered in the final quadratic equation to investigate the effect of independent variables on removal efficiency of Cr(VI):

$$Y = 56.87 + 1.22A + 9.16B - 5.59C - 5.86D + 2.35AB - 2.81AC - 1.69AD + 1.27BC + 2.48C^2 + 5.10D^2. \quad (6)$$

The scale of the effectiveness of single and interaction effects is p value < 0.05 [38]. Accordingly, all the linear terms (A, B, C, and D), four interaction terms (AB, AC, AD, and BC), and two quadratic terms (C^2 and D^2) were statistically significant as shown by results of ANOVA analysis. The remaining terms (BD, DC, A^2, and B^2) were not statistically significant.

In the response model equation, the factors that have a positive effect on the removal of Cr(VI) were A, B, AB, BC, CD, C^2, and D^2. The factors that have a negative effect on the removal of Cr(VI) were C, D, AC, and AD. The model equation selected for Cr(VI) removal was further analyzed using ANOVA component of the software to validate the importance and adequacy of the model. In Table 6, the model terms for responses have p value < 0.05 and F values of 84.21. The model $p < 0.05$ reveals that it is highly significant, and the higher F value of the model indicates that the model terms have the most significant effect on the removal of Cr(VI) from aqueous solution. The significant model terms in response surface quadratic model for Cr(VI) removal were found to be A, B, C, D, AB, AC, AD, BC, C^2, and D^2. B was the most significant model term on the Cr(VI) removal with F value of 497.56. The effect of the model terms on the removal of Cr(VI) are in the following order: B > D > C > D^2 > C^2 > AC > AB > AD > BC > A. The highest F value of 753.27 which corresponds to the effect of contact time on Cr(VI) removal indicates that the contact time is the most effective variable on Cr(VI) removal. It was observed that the lack of fit was not significant as p value > 0.05 indicating that the model is significant and valid [35].

3.7.1. Effect of Adsorbent Dosage and Initial Cr(VI) Ion Concentration on Removal of Cr(VI). Magnetic zeolite dosages of 0.40, 0.80, 1.2, 1.60, and 2.0 mg/L were used to investigate the effect of adsorbent dose on the adsorptive removal of Cr(VI) ions from aqueous solution. The effectiveness of adsorption process can be improved by increasing the adsorbent dose as more adsorbent provides larger active sites for adsorption. However, the effectiveness of adsorption does

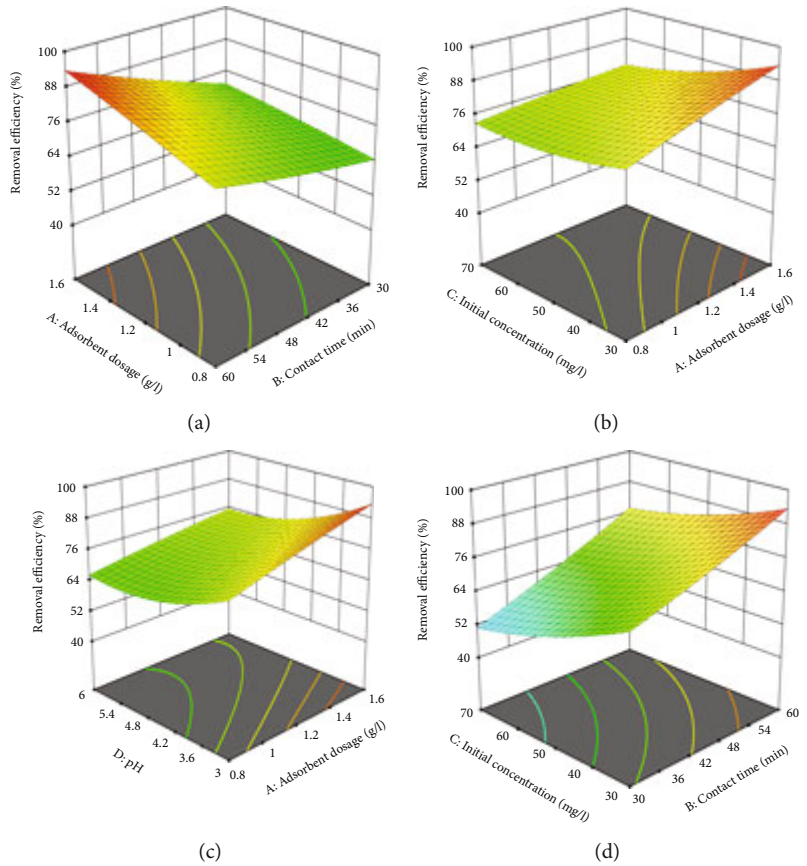

Figure 7: 3D response curve for interaction between adsorbent dose and contact time (AB), adsorbent dose and initial concentration (AC), adsorbent dose and pH (AD), and contact time and initial concentration (BC).

not depend on the adsorbent beyond the equilibrium dose as all adsorbents become adsorbed and non-left in solution [20]. In this study, adsorbent dose had a positive impact on the adsorptive removal of Cr(VI) in the range studied. The simultaneous effect of the adsorbent dose and initial Cr(VI) concentration on Cr(VI) removal by the magnetic zeolite is shown in Figure 7(b). The percentage of Cr(VI) removal increased with increasing adsorbent dose and initial Cr(VI) concentration. The dose had a positive significant interactive relationship with the initial Cr(VI) concentration for the magnetic zeolite.

3.7.2. Effect of Adsorbent Dosage and Contact Time on Removal of Cr(VI). Contact time is the most important parameters that influence adsorption process [46]. Removal efficiency can be increased by increasing the contact time until it reaches equilibrium time (a time at which no significant amount of adsorbate can be removed). The initial rapid uptake of adsorbate can be due to the presence of large number of vacant sites on the surface of adsorbent. As the time passes, effectiveness of adsorption reaches a constant value beyond which no more ions can occupy the active sites. This is due to the full occupation of vacant sites by the adsorbate [20]. In the current study, the effect of contact time on the adsorption removal of Cr(VI) was studied at contact time (15-75 min). The rate at which equilibrium can be achieved may signal the practical application of the adsorbent in the removal of Cr(VI) [48]. The positive coefficient of contact time indicates that increasing it increases Cr(VI) adsorption efficiencies in the studied range until it reaches equilibrium time. The highest F value of 497.56 which is related to the effect of contact time on Cr(VI) adsorption indicates that the contact time is the most effective variable in Cr(VI) adsorption. The dose exerted a negative impact in quadratic term for the magnetic zeolite.

3.7.3. Effect of Contact Time and Initial Cr(VI) Ion Concentration on Removal of Cr(VI). Batch adsorption experiments were conducted at different contact times (15, 30, 45, 60, and 75 min) and different initial concentrations of Cr(VI) (10, 30, 50, 70, and 90 mg/L) at optimum solution pH of 1.5 to investigate the interaction effect of contact time and initial Cr(VI) concentration on the removal of Cr(VI) ions. Increasing initial Cr(VI) concentration promotes adsorption since the interaction between adsorbate and adsorbent (magnetic zeolite) surface takes place effectively. However, when the initial concentration exceeds equilibrium concentration, adsorption cannot be improved because the surface of the adsorbent might be fully occupied by adsorbate and no space left for uptake [6]. The obtained ANOVA results revealed that the contact time is the most significant variable affecting the removal efficiency of Cr(VI)

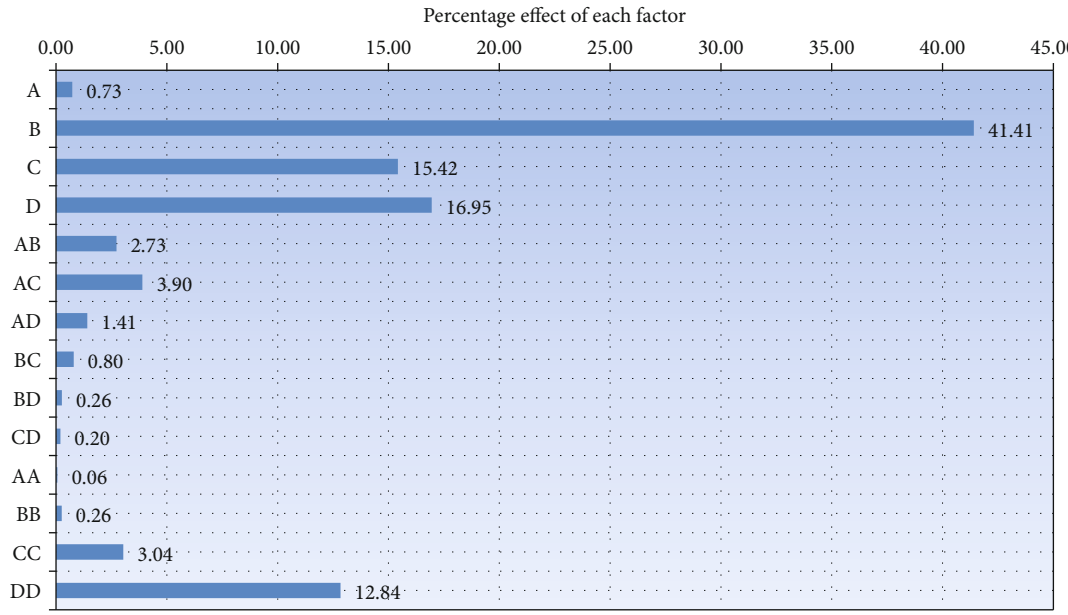

Figure 8: Pareto chart of the main effects of each term on the removal of Cr(VI).

($p < 0.0001$), followed by the solution pH ($p < 0.0001$) and initial Cr(VI) concentration ($p < 0.0001$) for the magnetic zeolite adsorbent.

3.7.4. Effect of Adsorbent Dosage and Solution pH on Removal of Cr(VI). The pH of the solution influences the dissociation of the active functional groups on the adsorbent surface and metal ion speciation in aqueous solution. To determine the optimum pH for the adsorption of Cr(VI) ions by magnetic zeolite from aqueous solution, experiments were conducted at pH 1.5, 3, 4.5, 6, and 7.5. The effect of pH is important in the adsorption process as it affects the solubility of metal ions, adsorbent surface charge, degree of ionization, and speciation [12]. The significant negative value for the interactive variables of the adsorbent dosage and solution pH for the magnetic zeolite indicate that there exist relationship between these variables (i.e., a change in one variable affects the other variable ($p = 0.0043$)). The combined effect of adsorbent dosage and solution pH on adsorption efficiency can be obtained from the plot shown in Figure 7(c).

Cr(VI) removal is shown to be very sensitive to pH variation, both at low and high adsorbent doses. Increasing the solution pH from an acidic level to near neutral (3 to 6) improved the Cr(VI) adsorption process. The influence of the pH on the adsorption of Cr(VI) ion by the magnetic zeolite could be indicated by considering the chemistry of the adsorbent surface as evidenced by the estimated pH_{PZC}. The magnetic zeolite had point of zero charge of 3.47. This suggests that a positive charge of the adsorbent was maintained until solution pH levels of <3.47, after which the charge of the adsorbent became negative. As a result, the surfaces of the adsorbent were completely protonated at a low $pH < pH_{PZC}$. This suggests that there exists electrostatic repulsion between Cr(VI) ions and the surface of adsorbent, resulting in decreased Cr(VI) adsorption onto the magnetic zeolite surfaces. When the pH was raised to 6, there occurred a considerable decrease in the number of positively charged adsorption sites, which was confirmed by the continuous increase in the Cr(VI) adsorption capacity of the magnetic zeolite.

In this study, the effect of variables affecting the adsorption process was investigated by a standardized Pareto diagram. Pareto analysis was used to predict the percentage effect of each independent variable on the removal of Cr(VI) from aqueous solution. The percentage effect of each parameter on the response (Cr(VI) removal) was calculated using the Pareto analysis (Pi) of the four independent variables:

$$Pi\,(\%) = \left(\frac{\beta i^2}{\sum \beta i^2}\right) x100 i \neq 0. \quad (7)$$

where βi is the regression coefficient of each parameter in the quadratic model equation in terms of coded factors.

The contribution of each variable on the removal of Cr(VI) is found different. The most influential independent variable and interaction effect on the response were found to be contact time (B) and pH ∗ pH (D^2), respectively (Figure 8). Among the four independent variables, 86.40% of the effects on response of the model is due to contact time (41.41%), solution pH (16.95%), initial concentration of Cr(VI) (15.42%), and pH ∗ pH (12.84%).

3.8. Optimization and Validation of the of Optimum Values. The optimization of removal efficiency with the highest desirability and process variables were carried out using Stat-Ease Design Expert Software version 13. The experimental conditions for the optimum removal of Cr(VI) using the recoverable magnetic zeolite were as follows: (A) adsorbent dose = 1.6 g/L, (B) contact time = 60 min, (C) initial concentration = 30 mg/L, and (D) pH = 3. The

Table 9: Validation of adsorption process variables under optimum conditions.

Constraint	Goal	Lower limit	Upper Limit	Lower weight	Upper weight	Importance
Adsorbent dose	In range	0.4	2	1	1	3
Contact time	In range	15	75	1	1	3
Initial conce.	In range	10	90	1	1	3
pH	In range	1.5	7.5	1	1	3
Removal efficiency	Maximize	38.88	94.88	1	1	3
Solution						
Solution number	Adsorbent dose (mg/L)	Contact time (min)	Initial conc. (mg/L)	pH	Removal efficiency (%)	Desirability	Status
1	2	75	10	1.5	93.57	0.977	**Selected**

Table 10: Comparison of optimum process variables and removal efficiency using experimental and software predictions.

Optimization	Optimum process variables				Optimum removal efficiency (%)
	Adsorbent dose (%)	Contact time (min)	Initial conc. (mg/L)	pH	
Experimental	1.6	60	30	3	94.88
Predicted	2	75	10	1.5	93.57

Table 11: Removal efficiency and cost for removal.

Adsorbent	Adsorbent cost for unit g Cr(VI) removal (USD)	Reference
Magnetic zeolite	0.01	Current study
Banana peels	0.42	[49]
Activated carbon	8.00	[49]
Pea pod peelings	0.53	[49]
Mixed tea and ginger waste	0.46	P. K. [49]
Natural zeolite	0.75	[49]
CSC coated with chitosan	0.25	P. K. [49]

Table 12: Adsorption isotherms of Cr(VI) ion adsorption.

C_o (mg/L)	C_e (mg/L)	$C_{o-}C_e$ (mg/L)	q_e (mg/g)	$\frac{Ce}{qe}$	log C_e	log q_e
10	0.69	9.31	5.82	0.1186	-0.112	0.7649
20	1.18	18.82	11.77	0.1003	0.072	1.0708
30	1.54	28.46	17.79	0.00.09	0.188	1.2502
40	3.20	36.8	23.00	0.1391	0.5051	1.3617
50	6.51	43.49	27.18	0.2391	0.8136	1.4343
60	9.08	50.92	31.82	0.2854	0.9581	1.5027
70	15.39	54.61	34.13	0.4509	1.1872	1.5331
80	20.11	59.89	37.43	0.5373	1.3034	1.5732
90	26.41	63.59	39.75	0.6644	1.4218	1.5993

removal efficiency Cr(VI) under these operating conditions was found to be 94.88%. The regression equation (Equation (6)) was solved using the Design Expert® 13 software to obtain optimal values for the four independent process variables and removal efficiency. The goal of each independent variable was set to "in range," while it was set to "maximize" for removal efficiency. In addition, both the lower and upper weights were set to 1, while importance was set at 3 as shown in Table 9. After looking for 100 solutions, the software displayed the optimum process variables and removal efficiency with the highest desirability.

The predicted optimal values for the four variables obtained from the software were adsorbent dose = 2 mg/L, contact time = 75 min, initial concentration = 10 mg/L, and pH = 1.5. The model predicted that the maximum removal efficiency under these optimum conditions is 93.57% which is very close to the experimental result as shown in Table 10. Therefore, the developed model was reliable and accurate for the prediction of Cr(VI) removal efficiency by the magnetic zeolite adsorbent.

Cost evaluation is a very useful tool to decide and fix the application of any physical and chemical processes. Economic costs and economic issues are important to select a process for the adsorptive removal of Cr(VI) or any other heavy metals from wastewater. Although the literature are over flooded with the different adsorbents for the removal of Cr(VI) from aqueous solution or industrial wastewater and economic evaluation, those methods are highly limited. The economic costs of an adsorption process mainly depend on the cost of the adsorbent used. Although activated carbon from various sources has been studied for long period of time to remove of Cr(VI) from aqueous solution or industrial wastewater, it is very expensive and unaffordable especially for economically under developed countries such as Ethiopia. Thus, an environmentally friendly, locally available, efficient, and economically feasible adsorbent material must be a prime objective in selecting adsorbent for the removal of heavy metals (Table 11).

3.9. Adsorption Isotherm and Kinetic Studies

3.9.1. Adsorption Isotherms. Adsorption isotherm relates the amount of adsorbate adsorbed by the adsorbent (q_e) with its

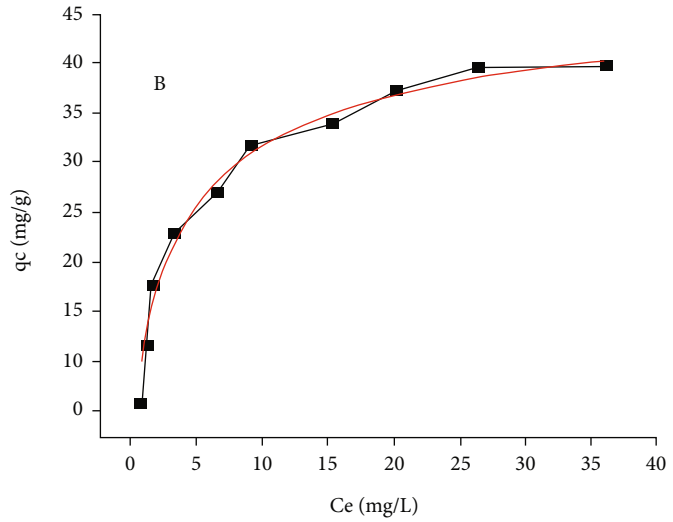

Figure 9: Nonlinear Langmuir isotherm model fitting for Cr(VI) ion adsorption.

Table 13: The Langmuir and Freundlich adsorption isotherms.

Langmuir isotherm					Freundlich isotherm		
q_m (mg/g)	R_L	b (L.mg^{-1})	R^2	K_F (mg/g) (L/mg)$^{1/nF}$	n	$1/n$	R^2
43.933	0.254 - 0.037	0.29347	0.9966	12.476	3.15	0.3175	0.92566

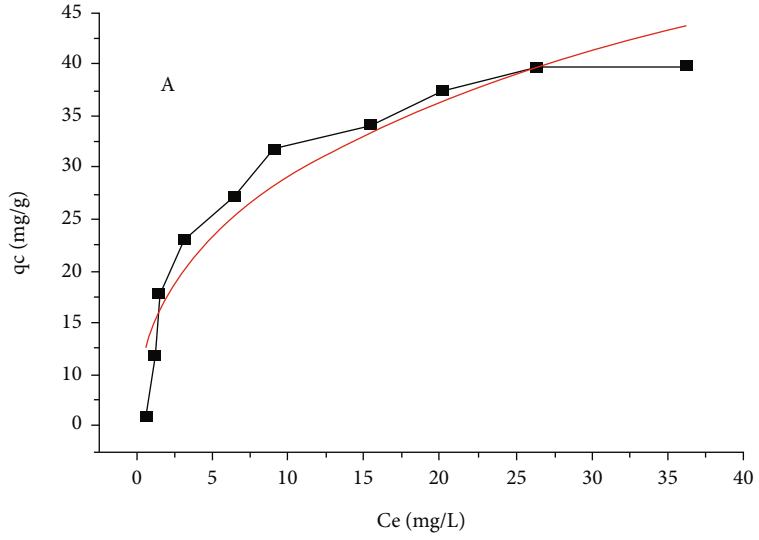

Figure 10: Freundlich nonlinear fitting of adsorption isotherm for Cr(VI) ion adsorption.

equilibrium concentration (C_e) in a solution at a specific temperature [40, 50]. Adsorption isotherm can be approached based on the data of initial concentration (C_o), concentration in solution at equilibrium (C_e), and equilibrium adsorption capacity (q_e) (Table 12). Many adsorption isotherm models have been developed though the Freundlich and Langmuir isotherm models are the most commonly used models. Langmuir isotherm model involves monolayer adsorption of adsorbate on the adsorbent surface having a limited number of identical adsorption sites without interacting with adsorbed ions, but in the Freundlich isotherm model, the adsorbate molecules form multilayers on the adsorbent surface due to the different affinities for various active sites and heterogeneous adsorbent surface [4, 21]. The nonlinear forms of Freundlich and Langmuir isotherm models are as follows [21]:

$$q_e = K_F C_e^{1/nF}, \tag{8}$$

$$q_e = \frac{q_m b C_e}{1 + bC_e}, \tag{9}$$

Table 14: Laboratory data for adsorption of Cr(VI) kinetics models.

Run	Time (min)	C_o (mg/l)	C_e (mg/l)	q_t	ln $(qe - qt)$	t/q_t
1.	5	30	12.258	11.09	1.90	0.45
2.	10	30	11.634	11.48	1.84	0.87
3.	15	30	10.947	11.91	1.77	1.26
4.	20	30	10.1964	12.38	1.69	1.62
5.	25	30	9.384	12.89	1.59	1.94
6.	30	30	8.508	13.43	1.47	2.23
7.	40	30	6.567	14.65	1.15	2.73
8.	50	30	4.374	16.02	0.58	3.12
9.	60	30	1.536	17.79	-4.61	3.37

Table 15: The adsorption kinetic parameters.

Pseudo-first order (PFO)			Pseudo-second order (PSO)		
q_e (mg/g)	k_1 (min^{-1})	R^2	q_e ($mg.g^{-1}$)	k_2 ($g.mg^{-1}\ min^{-1}$)	R^2
0.48	5.59	0.994	20.124	$7.64x10^{-4}$	0.968

In the current study, the adsorption isotherm experiments were conducted at the optimal conditions (i.e., adsorbent dose of 2.0 g/L, contact time 75 min, and solution pH 1.50) and at various initial Cr(VI) concentrations (i.e., 10.0, 20.0, 30.0, 40.0, 50.0, 60.0, 70.0, 80.0, and 90.0 mg/L). The Langmuir and Freundlich isotherm models were used to study the adsorption of Cr(VI) ions on the magnetic zeolite. The parameters for adsorption isotherm models were calculated using nonlinear regressions. The best fit isotherm model to the equilibrium data was chosen based on the coefficient of determination (R^2) which measures how well the predicted values of the model match with the experimental data [3]. The constants in the Freundlich isotherm model were determined by plotting log C_e against log q_e in which log KF is intercept and $1/n$ is slope of the curve (Figure 9). The curve was used to fit experimental data to the appropriate isotherm model, and the values of intercept (log K_F) and slope ($1/n$) were determined from this curve using nonlinear regression analysis. The K_F and n values of Freundlich model for this study were found to be 12.48 and 3.15, respectively (Table 13). The value of $1/n$ indicates the adsorption intensity or surface heterogeneity which ranges between 0 and 1 [21]. If the value of $1/n$ approaches unity, it indicates that just a little concentration change can affect the adsorption process. If $n < 1$, the adsorbent can effectively adsorb the adsorbate. When n value exceeds 2 but not greater than 10, the adsorption process is easy to proceed. However, the adsorption is too weak if $n < 0.50$ [43]. The value of $n = 3.15$ for this study revealed that the adsorption process can easily proceed without any difficulty. The value of $1/n = 0.3175$ lies between 0 and 1, suggesting that the magnetic zeolite adsorbs Cr(VI) ions effectively from aqueous solution.

The constants in the Langmuir isotherm model can be determined by plotting C_e (mg/L) against C_e/q_e in which the intercept is $1/bq_m$ and slope is $1/q_m$ (Figure 10). In this isotherm equation, q_m (mg/g) is the maximum monolayer adsorption capacity, while b (L/mg) is the Langmuir adsorption intensity constant which indicates the affinity of adsorbent towards adsorbate [21]. The calculated isotherm parameters are given in Table 13. For the adsorption of Cr(VI) ions by magnetic zeolite, the Langmuir constants q_m and b were found to be 43.933 mg/g and 0.29347, respectively. The value of q_m indicates one gram of magnetic zeolite can adsorb 43.933 mg of Cr(VI) ions from aqueous solution at equilibrium. The coefficients of determination (R^2) of the Langmuir isotherm model for Cr(VI) ion removal was found to be 0.9966, indicating that the experimental data best fit to Langmuir isotherm model. It suggests that the monolayer Cr(VI) ions were formed on the surface of the magnetic zeolite. Therefore, each site of the magnetic zeolite can be characterized by having a heterogeneous surface. The conformity of the adsorption process to the Langmuir isotherm model can be expressed by a dimensionless constant of separation factor (R_L) (Equation (8)) in which the value of R_L gives an idea about the shape of isotherm [35]. The effect of the isotherm shape can be used to predict if an adsorption system is favorable, unfavorable, linear, or irreversible. The parameter R_L (Equation (8)) indicates the shape of the isotherm:

$$R_L = \frac{1}{1 + bC_o}, \tag{10}$$

where C_o (mg/L) is the initial adsorbate concentration and b (L/mg) is the Langmuir constant which is related to the energy of adsorption. The value of R_L indicates the nature of adsorption process ($R_L > 1$: adsorption process is unfavorable; $R_L = 1$: adsorption is linear; $0 < R_L < 1$: adsorption process is favorable; and $R_L = 0$: adsorption is irreversible). The R_L value lies between 0 and 1 for the current study (R_L varied between 0.2541 and 0.0365), suggesting that the adsorption process is favorable under the studied conditions. This shows that magnetic zeolite is a good adsorbent in removing Cr(VI) ions from aqueous solution.

3.9.2. Adsorption Kinetics. Adsorption kinetics describes the rate controlling the contact time of adsorption of adsorbate onto adsorbent at solid/solution interface. The design of an adsorption system requires the rate of adsorption for the given system [35]. Kinetics study gives information about the factors controlling the reaction rate and adsorption mechanism [39]. The pseudo-first-order (PFO), pseudo-second-order (PSO), and intraparticle diffusion (IPD) kinetic models may be used to assess the kinetic parameters of the adsorption process (Table 14). However, PFO and PSO kinetic models are the most commonly used models to express the relationship between adsorption of adsorbates and the amount of available binding sites on the surface of the adsorbent [4]. The PSO model represents that the rate-controlling step for the adsorption process involves chemisorption by covalent forces or ion

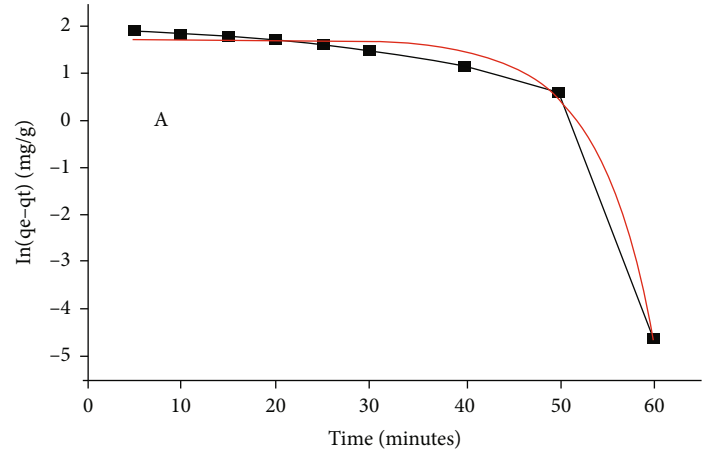

Figure 11: Nonlinear fitting of PFO kinetic for Cr(VI) ion adsorption from aqueous solution.

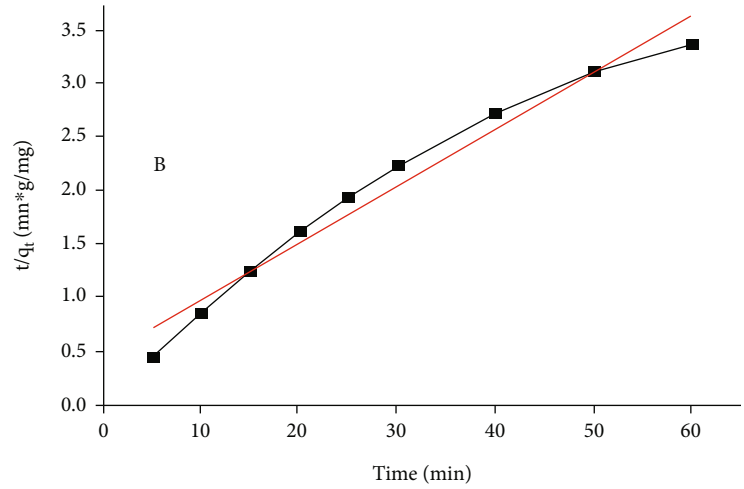

Figure 12: Nonlinear fitting of PSO kinetic for Cr(VI) ion adsorption from aqueous solution.

exchange. In this study, adsorption kinetic parameters were determined based on the contact time variation using PFO and PSO kinetic models. The nonlinear and linearized forms of PFO and PSO kinetic models are expressed as follows [15]:

$$\ln(q_e - q_t) = \ln q_{e-\left(\frac{k_1}{2.303}\right)t},$$
$$\frac{t}{q_t} = \frac{1}{q_e^2 k_2} + \frac{t}{q_e}, \quad (11)$$

where q_e (mg.g^{-1}) and q_t (mg.g^{-1}) are, respectively, the amounts of adsorbate adsorbed at equilibrium and at any instant of time t (min), while k_1 (min^{-1}) and k_2 (g/mg.min) are, respectively, PFO and PSO rate constants. A nonlinear regression was used for nonlinear curve fitting to calculate the kinetic model parameters. The parameters obtained were adsorption capacity at equilibrium (q_e) and adsorption rate constant (k_i) (Table 15).

The quantity of kinetic parameters, q_e and k_1, of the PFO model were determined from the intercept and slope of the curve $\ln(q_e - q_t)$ against t, respectively (Figure 11). On the other hand, the parameters, adsorption rate constant (k_2), and equilibrium adsorption capacity (q_e) of the PSO model were, respectively, calculated from the intercept and slope of the curve t/q_t against t (min) (Figure 12). A comparison of experimental adsorption capacities (q_e) and kinetic constants (k_1 and k_2) of the magnetic zeolite adsorbent obtained for the PFO and PSO kinetic models are shown in Table 15. The rate constant k_1 and coefficient of determination value for the PFO model were found to be 5.59 min^{-1} and 0.994, respectively, for the magnetic zeolite adsorbent. The studies on the adsorption of Cr(VI) onto magnetic zeolite revealed that the adsorption process fitted to the PFO kinetic model. The R^2 value obtained from the model is more than R^2 (0.968) value of the PSO kinetic model. The adsorption capacity of PSO was found to be 20.124 mg/g with the adsorption rate constant, q_e of 7.64×10^{-4} g mg^{-1} min^{-1} that show good ability of the adsorbent and its promising potential for the removal of Cr(IV) ion wastewater.

Table 16: Maximum adsorption capacity of various adsorbents for Cr(VI) removal from aqueous solutions.

Adsorbent	q_m (mg/g)	Reference
Coconut husk fiber	29.0	[51]
Leaf mold	25.90	D. C. [52]
Coffee husk	2.04	[43]
Sugar cane bagasse	13.40	D. C. [52]
Palm pressed-fibers	15.0	[51]
Neem leaves	63.0	[53]
Eucalyptus bark	45.0	[54]
Cactus	7.08	[54]
Chitosan cross-epichlorohydrin	11.30	[32, 55]
Ocimum americanum L. seed pods	83.30	[56]
Activated carbon	69.30	[57]
Cydonia oblonga	83.30	[15]
Modified clay mineral	10.0	[9]
Amine-functionalized zeolite	13.50	[58]
Zeolites	26.00	[59]
Leucaena leucocephala seed pod activated carbon	26.94	[60]
Magnetic zeolite	43.93	Current study

The maximum adsorption capacity of the magnetic zeolite for Cr(VI) adsorption has been compared with other adsorbents reported in the literature (Table 16). Comparison of the maximum adsorption capacity (q_m) of magnetic zeolite with various adsorbents revealed that the magnetic zeolite has high adsorption capacity than many of the adsorbents. The result of the current study indicates that the magnetic zeolite adsorbent has a good adsorption capacity.

4. Conclusions

The adsorptive removal of Cr(VI) from aqueous solution was carried out in a batch experiment with a natural zeolite coated with magnetic nanoparticles (Fe_3O_4) to improve its surface characters, recoverability, adsorption capacity, and removal efficiency. The FTIR spectra analysis revealed that the magnetic zeolite contains functional groups such as hydroxyl (O-H-O), Fe-O, and O-Si-O/O-Al-O participating on Cr(VI) binding onto the surface of the magnetic zeolite. The CCD with five level-four factor was used to design 30 batch experiments in order to determine optimum adsorption process variables for the maximum removal of Cr(VI) using the magnetic zeolite. The optimization of experimental results by RSM revealed that adsorbent dose of 2 g/L, contact time of 75 min, initial Cr(VI) concentration of 10 mg/L, and solution pH of 1.5 were the optimum adsorption process variables to achieve a maximum removal efficiency of 93.57%. The Langmuir and Freundlich isotherm models were used to describe the adsorption isotherm. The Langmuir isotherm shows a better fit to the process with $R^2 = 0.9966$ and adsorption capacity of 43.933 mg/g. The study of adsorption kinetics revealed that equilibrium in the adsorption of Cr(VI) ion reaches in 75 min of contact between the magnetic zeolite and the solution. The study of adsorption kinetics parameters revealed that the kinetics of the adsorption of Cr(VI) onto magnetic zeolite follows the PFO. The n value in Freundlich model was greater than unity, indicating that the adsorption of Cr(VI) ions onto magnetic zeolite is favorable. The adsorption of Cr(VI) ions on the magnetic zeolite well fits to PFO model with rate constant of 5.59 (min^{-1}). The magnetic zeolite has the potential to be used as an efficient and cost-effective adsorbent for the removal of Cr(VI) ions from industrial effluents. As future prospects, magnetic zeolite prepared by Sonolysis, Sogel, and impregnation techniques must be studied to compare the findings with the current study. Also, the use of alternate experimental methods other than the batch method needs to be investigated for the removal of Cr(VI) ions from aqueous solution using the magnetic natural zeolite. A further study is needed to validate the finding of the current study in the removal of hexavalent chromium from a real industrial wastewater.

Data Availability

All data, models, and codes generated or used during this study are available in this article.

Conflicts of Interest

All authors declare that they have no conflicts of interest.

Acknowledgments

The authors are very grateful to Jimma University, Jimma Institute of Technology, office of Research and Publication and ExiST project: Excellence in Science and Technology, Ethiopia, funded by KfW, Germany, through Jimma Institute of Technology, Center of Excellence for providing financial assistance to conduct the study (RPD3720).

References

[1] A. H. Mahvi and E. Bazrafshan, "Remarkable reusability of magnetic Fe 3 O 4- graphene oxide composite : a highly effective adsorbent for Cr (VI) ions," *International Journal of Environmental Analytical Chemistry*, vol. 101, pp. 1–21, 2021.

[2] B. Alawa, J. K. Srivstava, A. Srivastava, and J. Palsania, "Adsorption of heavy metal Pb (II) from synthetic waste water by polypyrrole composites," *International Journal of Chemical Studies*, vol. 3, no. 1, pp. 4–8, 2015.

[3] M. Fazlzadeh, K. Rahmani, A. Zarei, H. Abdoallahzadeh, F. Nasiri, and R. Khosravi, "A novel green synthesis of zero valent iron nanoparticles (NZVI) using three plant extracts and their efficient application for removal of Cr(VI) from aqueous solutions," *Advanced Powder Technology*, vol. 28, no. 1, pp. 122–130, 2017.

[4] M. Hadi, A. Zarei, and A. Mesdaghinia, "Adsorption of Cr (VI) ions from aqueous systems using thermally sodium organobentonite biopolymer composite (TSOBC): response surface methodology, isotherm, kinetic and thermodynamic studies," *Desalination and Water Treatment*, vol. 85, pp. 298–312, 2017.

[5] M. Farrokhi, M. Naimi-Joubani, A. Dargahi, M. Poursadeghiyan, and H. Ali Jamali, "Investigating activated sludge microbial population efficiency in heavy metals removal from compost leachate," *Polish Journal of Environmental Studies*, vol. 27, no. 2, pp. 623–627, 2018.

[6] A. Gaffer, A. A. Al Kahlawy, and D. Aman, "Magnetic zeolite-natural polymer composite for adsorption of chromium (VI)," *Egyptian Journal of Petroleum*, vol. 26, no. 4, pp. 995–999, 2017.

[7] A. Dargahi, H. Golestanifar, P. Darvishi et al., "An investigation and comparison of removing heavy metals (Lead and chromium) from aqueous solutions using magnesium oxide nanoparticles," *from Aqueous Solutions Using Magnesium Oxide Nanoparticles.*, vol. 25, no. 2, pp. 557–562, 2016.

[8] G. Nagpal, A. Bhattacharya, and N. B. Singh, "Removal of chromium(VI) from aqueous solution by carbon waste from thermal power plant," *Desalination and Water Treatment*, vol. 57, no. 21, pp. 9765–9775, 2016.

[9] E. A. Ashour and M. A. Tony, "Eco-friendly removal of hexavalent chromium from aqueous solution using natural clay mineral: activation and modification effects," *SN Applied Sciences*, vol. 2, no. 12, pp. 1–13, 2020.

[10] S. Abdel, A. Monem, M. Ahmed, M. S. Adam, and M. A. Mohamed, "Adsorption studies on the removal of hexavalent chromium-contaminated wastewater using activated carbon and bentonite," *Chemistry Journal*, vol. 2, no. 3, pp. 95–105, 2012.

[11] A. S. Hamouda, S. A. Ahmed, N. M. Mohamed, and M. M. H. Khalil, "Adsorption of chromium(VI) from aqueous solution by glycine modified cross-linked chitosan resin," *Egyptian Journal of Chemistry*, vol. 61, pp. 799–812, 2018.

[12] O. Ajouyed and C. Hurel, "Evaluation of the adsorption of hexavalent chromium on kaolinite and Illite," *Journal of Environmental Protection*, vol. 2, no. 10, pp. 1347–1352, 2011.

[13] M. Mwinyihija, "Main Pollutants and Environmental Impacts of the Tanning Industry," in *Ecotoxicological Diagnosis in the Tanning Industry*, pp. 17–35, Springer, New York, NY, 2010.

[14] S. K. Upadhyay, M. Tripathi, M. Kaur, and K. Kaur, "Toxicity concerns of hexavalent chromium from tannery waste," *Journal of Biotechnology and Bioengineering V2*, vol. 2, no. 2, p. 40, 2018.

[15] E. Bazrafshan, M. Sobhanikia, F. K. Mostafapour, H. Kamani, and D. Balarak, "Chromium biosorption from aqueous environments by mucilaginous seeds of Cydonia oblonga: kinetic and thermodynamic studies," *Global NEST Journal*, vol. 19, no. 2, pp. 269–277, 2019.

[16] A. Almasi, A. Dargahi, M. Mohammad, H. Ahagh, and M. Mohammadi, "Efficiency of a constructed wetland in controlling organic pollutants, nitrogen, and heavy metals from sewage," *Journal of Chemical and Pharmaceutical Sciences*, vol. 9, no. 4, pp. 2924–2928, 2016.

[17] Y. Y. Li, T. T. Zhang, Z. Ning, and J. H. Chen, "Characteristics and applications of sewage sludge biochar modified by ferrous sulfate for remediating Cr(VI)-contaminated soils," *Advances in Civil Engineering*, vol. 2020, Article ID 6521638, 10 pages, 2020.

[18] B. An, "Cu(II) and As(V) adsorption kinetic characteristic of the multifunctional amino groups in chitosan," *PRO*, vol. 8, no. 9, p. 1194, 2020.

[19] B. Rzig, F. Guesmi, M. Sillanpää, and B. Hamrouni, "Modelling and optimization of hexavalent chromium removal from aqueous solution by adsorption on low-cost agricultural waste biomass using response surface methodological approach," *Water Science and Technology*, vol. 84, no. 3, pp. 552–575, 2021.

[20] T. Dula, K. Siraj, and S. A. Kitte, "Adsorption of hexavalent chromium from aqueous solution using chemically activated carbon prepared from locally available waste of bamboo (Oxytenanthera abyssinica)," *ISRN Environmental Chemistry*, vol. 2014, Article ID 438245, 9 pages, 2014.

[21] Z. Alhalili, "Green synthesis of copper oxide nanoparticles CuO NPs from _Eucalyptus Globoulus_ leaf extract: Adsorption and design of experiments," *Arabian Journal of Chemistry*, vol. 15, no. 5, p. 103739, 2022.

[22] V. Hernández-Montoya, M. A. Pérez-Cruz, D. I. Mendoza-Castillo, M. R. Moreno-Virgen, and A. Bonilla-Petriciolet, "Competitive adsorption of dyes and heavy metals on zeolitic structures," *Journal of Environmental Management*, vol. 116, pp. 213–221, 2013.

[23] A. Nasiri, S. Rajabi, and M. Hashemi, "CoFe 2 O 4 @ methylcellulose/AC as a new, green, and eco-friendly nano-magnetic adsorbent for removal of reactive red 198 from aqueous solution," *Arabian Journal of Chemistry*, vol. 15, no. 5, p. 103745, 2022.

[24] M. Stefan, C. Leostean, O. Pana et al., "Synthesis and characterization of Fe 3 O 4 @ZnS and Fe 3 O 4 @Au@ZnS core-shell nanoparticles," *Applied Surface Science*, vol. 288, no. 1, pp. 180–192, 2014.

[25] M. Mahreni, R. Ramadhan, M. Pramadhana, A. Permatasari, D. Kurniawati, and H. Kusuma, "Synthesis of metal organic framework (MOF) based Ca-alginate for adsorption of malachite green dye," *Polymer Bulletin*, vol. 79, no. 1, 2022.

[26] M. A. Barakat, "New trends in removing heavy metals from industrial wastewater," *Arabian Journal of Chemistry*, vol. 4, no. 4, pp. 361–377, 2011.

[27] X. Xin, Q. Wei, J. Yang et al., "Highly efficient removal of heavy metal ions by amine-functionalized mesoporous Fe 3O 4 nanoparticles," *Chemical Engineering Journal*, vol. 184, pp. 132–140, 2012.

[28] M. M. Rahman, M. B. Awang, and A. M. Yusof, "Preparation, characterization and application of zeolite-Y (Na-Y) for water filtration," *Australian Journal of Basic and Applied Sciences*, vol. 6, no. 1, pp. 50–54, 2012.

[29] M. Solgi, T. Najib, S. Ahmadnejad, and B. Nasernejad, "Synthesis and characterization of novel activated carbon from Medlar seed for chromium removal: experimental analysis and modeling with artificial neural network and support vector regression," *Resource-Efficient Technologies*, vol. 3, no. 3, pp. 236–248, 2017.

[30] A. A. Mohammed and S. L. Kareem, "Adsorption of tetracycline fom wastewater by using pistachio shell coated with ZnO nanoparticles: equilibrium, kinetic and isotherm studies," *Alexandria Engineering Journal*, vol. 58, no. 3, pp. 917–928, 2019.

[31] Y. A. B. Neolaka, G. Supriyanto, H. Darmokoesoemo, and H. S. Kusuma, "Characterization, kinetic, and isotherm data for Cr(VI) removal from aqueous solution by Cr(VI)-imprinted poly(4-VP-co-MMA) supported on activated Indonesia (Ende-Flores) natural zeolite structure," *Data in Brief*, vol. 17, pp. 969–979, 2018.

[32] H. Liu, S. Peng, L. Shu, T. Chen, T. Bao, and R. L. Frost, "Magnetic zeolite NaA: synthesis, characterization based on metakaolin and its application for the removal of Cu^{2+}, Pb^{2+}," *Chemosphere*, vol. 91, no. 11, pp. 1539–1546, 2013.

[33] T. Pambudi, E. T. Wahyuni, and M. Mudasir, "Recoverable adsorbent of natural zeolite/Fe3O4 for removal of Pb (II) in water," *Journal of Materials and Environmental Sciences*, vol. 11, no. 1, pp. 69–78, 2020.

[34] A. Gupta, V. Sharma, K. Sharma et al., "A review of adsorbents for heavy metal decontamination: growing approach to wastewater treatment," *Materials*, vol. 14, no. 16, pp. 1–45, 2021.

[35] M. A. Fawzy, H. Darwish, S. Alharthi, M. I. Al-Zaban, A. Noureldeen, and S. H. A. Hassan, "Process optimization and modeling of Cd2+ biosorption onto the free and immobilized Turbinaria ornata using Box–Behnken experimental design," *Scientific Reports*, vol. 12, no. 1, pp. 1–18, 2022.

[36] M. Heidari, M. Vosoughi, H. Sadeghi, A. Dargahi, and S. A. Mokhtari, "Degradation of diazinon from aqueous solutions by electro-Fenton process: effect of operating parameters, intermediate identification, degradation pathway, and optimization using response surface methodology (RSM)," *Separation Science and Technology*, vol. 56, no. 13, pp. 2287–2299, 2021.

[37] M. R. Samarghandi, A. Ansari, A. Dargahi et al., "Enhanced electrocatalytic degradation of bisphenol A by graphite/β-PbO_2 anode in a three-dimensional electrochemical reactor," *Journal of Environmental Chemical Engineering*, vol. 9, no. 5, p. 106072, 2021.

[38] S. Alizadeh, H. Sadeghi, M. Vosoughi, A. Dargahi, and S. A. Mokhtari, "Removal of humic acid from aqueous media using Sono-Persulphate process: optimization and modelling with response surface methodology (RSM)," *International Journal of Environmental Analytical Chemistry*, vol. 100, pp. 1–15, 2020.

[39] A. Dargahi, M. R. Samarghandi, A. Shabanloo, M. M. Mahmoudi, and H. Z. Nasab, "Statistical modeling of phenolic compounds adsorption onto low-cost adsorbent prepared from aloe vera leaves wastes using CCD-RSM optimization: effect of parameters, isotherm, and kinetic studies," *Biomass Conversion and Biorefinery.*, vol. 11, 2021.

[40] A. Dalvand, M. Khoobi, R. Nabizadeh, M. Reza, and E. Gholibegloo, "Reactive dye adsorption from aqueous solution on HPEI-modified - Fe 3 O 4 nanoparticle as a superadsorbent : characterization, modeling, and optimization," *Journal of Polymers and the Environment*, vol. 26, no. 8, pp. 3470–3483, 2018.

[41] D. Beyene, M. Abdulkadir, and A. Befekadu, "Production of Biodiesel from Mixed Castor Seed and Microalgae Oils : Optimization of the Production and Fuel Quality Assessment," *Journal of Chemical Engineering*, vol. 2022, article 1536160, 14 pages, 2022.

[42] A. Seidmohammadi, Y. Vaziri, A. Dargahi, and H. Z. Nasab, "Improved degradation of metronidazole in a heterogeneous photo-Fenton oxidation system with PAC/Fe3O4 magnetic catalyst: biodegradability, catalyst specifications, process optimization, and degradation pathway," *Biomass Conversion and Biorefinery*, vol. 11, 2021.

[43] D. Abdissa, T. Abeto, and Y. Mekonnen, "Adsorptive capacity of coffee husk in the removal of chromium (VI) and zink (II) from tannery effluent : kinetics and equilibrium studies," *Water Conservation and Management (WCM)*, vol. 5, no. 2, pp. 54–60, 2021.

[44] M. Manjuladevi, R. Anitha, and S. Manonmani, "Kinetic study on adsorption of Cr(VI), Ni(II), cd(II) and Pb(II) ions from aqueous solutions using activated carbon prepared from Cucumis melo peel," *Applied Water Science*, vol. 8, no. 1, pp. 1–8, 2018.

[45] A. A. Werkneh, N. G. Haftu, and H. D. Beyene, "Removal of hexavalent chromium from tannery wastewater using activated carbon primed from sugarcane bagasse," *Adsorption/Desorption Studies*, vol. 2, no. 6, pp. 128–135, 2014.

[46] S. Afshin, Y. Rashtbari, M. Vosough et al., "Application of Box-Behnken design for optimizing parameters of hexavalent chromium removal from aqueous solutions using Fe_3O_4 loaded on activated carbon prepared from alga: Kinetics and equilibrium study," *Journal of Water Process Engineering*, vol. 42, no. April, p. 102113, 2021.

[47] A. Fakhri, "Application of response surface methodology to optimize the process variables for fluoride ion removal using maghemite nanoparticles," *Journal of Saudi Chemical Society*, vol. 18, no. 4, pp. 340–347, 2014.

[48] S. Babel and T. A. Kurniawan, "A research study on Cr(VI) removal from contaminated wastewater using natural zeolite," *Journal of Ion Exchange*, vol. 14, Supplement, pp. 289–292, 2003.

[49] P. K. Sharma and S. Ayub, "The cost analysis and economic feasibility of agro wastes to adsorb chromium (VI) from wastewater," *International Journal of Civil Engineering and Technology*, vol. 10, no. 2, pp. 2387–2402, 2019.

[50] A. Ali, K. Saeed, and F. Mabood, "Removal of chromium (VI) from aqueous medium using chemically modified banana peels as efficient low-cost adsorbent," *Alexandria Engineering Journal*, vol. 55, no. 3, pp. 2933–2942, 2016.

[51] W. T. Tan, S. T. Ooi, and C. K. Lee, "Removal of chromium(Vi) from solution by coconut husk and palm pressed fibres," *Environmental Technology*, vol. 14, no. 3, pp. 277–282, 1993.

[52] D. C. Sharma and C. F. Forster, "A preliminary examination into the adsorption of hexavalent chromium using low-cost adsorbents," *Bioresource Technology*, vol. 47, no. 3, pp. 257–264, 1994.

[53] B. V. Babu and S. Gupta, "Adsorption of Cr(VI) using activated neem leaves: kinetic studies," *Adsorption*, vol. 14, no. 1, pp. 85–92, 2008.

[54] V. Sarin and K. K. Pant, "Removal of chromium from industrial waste by using eucalyptus bark," *Bioresource Technology*, vol. 97, no. 1, pp. 15–20, 2006.

[55] B. Hastuti, A. Masykur, and S. Hadi, "Modification of chitosan by swelling and crosslinking using epichlorohydrin as heavy metal Cr (VI) adsorbent in batik industry wastes," *IOP Conference Series: Materials Science and Engineering*, vol. 107, no. 1, p. 012020, 2016.

[56] L. Levankumar, V. Muthukumaran, and M. B. Gobinath, "Batch adsorption and kinetics of chromium (VI) removal from aqueous solutions by Ocimum americanum L. seed pods," *Journal of Hazardous Materials*, vol. 161, no. 2–3, pp. 709–713, 2009.

[57] Z. Hu, L. Lei, Y. Li, and Y. Ni, "Chromium adsorption on high-performance activated carbons from aqueous solution," *Separation and Purification Technology*, vol. 31, no. 1, pp. 13–18, 2003.

[58] S. Nasanjargal, B.-A. Munkhpurev, N. Kano, H.-J. Kim, and Y. Ganchimeg, "The removal of chromium(VI) from aqueous solution by amine-functionalized zeolite: kinetics, thermodynamics, and equilibrium study," *Journal of Environmental Protection*, vol. 12, no. 9, pp. 654–675, 2021.

[59] V. Tare, S. Chaudhari, and M. Jawed, "Comparative evaluation of soluble and insoluble xanthate process for heavy metal removal from wastewaters," *Science and Technology*, vol. 26, no. 1-2, pp. 237–246, 1992.

[60] A. S. Yusuff, "Adsorption of hexavalent chromium from aqueous solution by Leucaena leucocephala seed pod activated carbon: equilibrium, kinetic and thermodynamic studies," *Arab Journal of Basic and Applied Sciences*, vol. 26, no. 1, pp. 89–102, 2019.